



Unification of Weak and EM form factors of octet baryons

Zhao-Qian Yao

In collaboration with
Craig D. Roberts, Daniele Binosi

Sept 20, 2023
ECT*, Trento

Electromagnetic and Weak form factors

- The study of electromagnetic form factors is crucial to understanding the substructure of hadrons, where a lot of theoretical and experimental efforts have been made.

Electromagnetic and Weak form factors

- The study of electromagnetic form factors is crucial to understanding the substructure of hadrons, where a lot of theoretical and experimental efforts have been made.

PRL **112**, 132503 (2014)

PHYSICAL REVIEW LETTERS

week ending
4 APRIL 2014

JLab Measurement of the ^4He Charge Form Factor at Large Momentum Transfers

A. Camsonne,²² A. T. Katramatou,¹¹ M. Olson,²⁰ N. Sparveris,^{11,21} A. Acha,⁴ K. Allada,¹² B. D. Anderson,¹¹ J. Arrington,¹ A. Baldwin,¹¹ J.-P. Chen,²² S. Choi,¹⁸ E. Chudakov,²² E. Cisbani,^{8,10} B. Craver,²³ P. Decowski,¹⁹ C. Dutta,¹² E. Folts,²² S. Frullani,^{8,10} F. Garibaldi,^{8,10} R. Gilman,^{16,22} J. Gomez,²² B. Hahn,²⁴ J.-O. Hansen,²² D. W. Higinbotham,²² T. Holmstrom,¹³ J. Huang,¹⁴ M. Iodice,⁹ X. Jiang,¹⁶ A. Kelleher,²⁴ E. Khrosinkova,¹¹ A. Kievsky,⁷ E. Kuchina,¹⁶ G. Kumbartzki,¹⁶ B. Lee,¹⁸ J. J. LeRose,²² R. A. Lindgren,²³ G. Lott,²² H. Lu,¹⁷ L. E. Marcucci,^{7,15} D. J. Margaziotis,² P. Markowitz,⁴ S. Marrone,⁶ D. Meekins,²² Z.-E. Meziani,²¹ R. Michaels,²² B. Moffit,¹⁴ B. Norum,²³ G. G. Petratos,¹¹ A. Puckett,¹⁴ X. Qian,³ O. Rondon,²³ A. Saha,²² B. Sawatzky,²¹ J. Segal,²² M. Shabestari,²³ A. Shahinyan,²⁵ P. Solvignon,¹ R. R. Subedi,²³ R. Suleiman,²² V. Sulkosky,²² G. M. Urciuoli,⁸ M. Viviani,⁷ Y. Wang,⁵ B. B. Wojtsekhowski,²² X. Yan,¹⁸ H. Yao,²¹ W.-M. Zhang,¹¹ X. Zheng,²³ and L. Zhu⁵

(The Jefferson Lab Hall A Collaboration)

Electromagnetic and Weak form factors

- The study of electromagnetic form factors is crucial to understanding the substructure of hadrons, where a lot of theoretical and experimental efforts have been made.

PRL 112, 132503 (2014)

JLab Measurement of

A. Camsonne,²² A. T. Katramatou,
A. Baldwin,¹¹ J.-P. Chen,²² S. Ch
S. Frullani,^{8,10} F. Garibaldi,⁸
T. Holmstrom,¹³ J. Huang,¹⁴ M
G. Kumbartzki,¹⁶ B. Lee,¹⁸ J. J.
P. Markowitz,⁴ S. Marrone,⁶ D.
A. Puckett,¹⁴ X. Qian,³ O. Rondor
R. R. Subedi,²³ R. Suleiman,²² V.

Article

A small proton charge radius from an electron–proton scattering experiment

<https://doi.org/10.1038/s41586-019-1721-2>

Received: 17 June 2019

Accepted: 19 September 2019

Published online: 6 November 2019

W. Xiong¹, A. Gasparian^{2*}, H. Gao¹, D. Dutta^{3*}, M. Khandaker⁴, N. Liyanage⁵, E. Pasyuk⁶, C. Peng¹, X. Bai⁵, L. Ye³, K. Gnanvo⁵, C. Gu¹, M. Levillain², X. Yan¹, D. W. Higinbotham⁶, M. Meziane¹, Z. Ye¹⁷, K. Adhikari³, B. Aljawrneh², H. Bhatt³, D. Bhetuwal³, J. Brock⁶, V. Burkert⁶, C. Carlin⁶, A. Deur⁶, D. Di⁵, J. Dunne³, P. Ekanayaka³, L. El-Fassi³, B. Emmich³, L. Gan⁸, O. Glamazdin⁹, M. L. Kabir³, A. Karki³, C. Keith⁶, S. Kowalski¹⁰, V. Lagerquist¹¹, I. Larin^{12,13}, T. Liu¹, A. Liyanage¹⁴, J. Maxwell⁶, D. Meekins⁶, S. J. Nazeer¹⁴, V. Nelyubin⁵, H. Nguyen⁵, R. Pedroni², C. Perdrisat¹⁵, J. Pierce⁶, V. Punjabi¹⁶, M. Shabestari⁶, A. Shahinyan¹⁷, R. Silwal¹⁰, S. Stepanyan⁶, A. Subedi³, V. V. Tarasov¹², N. Ton⁵, Y. Zhang¹ & Z. W. Zhao¹

Elastic electron–proton scattering (e–p) and the spectroscopy of hydrogen atoms are the two methods traditionally used to determine the proton charge radius, r_p . In 2010, a new method using muonic hydrogen atoms¹ found a substantial discrepancy compared with previous results², which became known as the ‘proton radius puzzle’. Despite experimental and theoretical efforts, the puzzle remains unresolved. In fact, there is a discrepancy between the two most recent spectroscopic measurements conducted on ordinary hydrogen^{3,4}. Here we report on the proton charge radius experiment at Jefferson Laboratory (PRad), a high-precision e–p experiment that was established after the discrepancy was identified. We used a magnetic-spectrometer-free method along with a windowless hydrogen gas target, which overcame several limitations of previous e–p experiments and enabled measurements at very small forward-scattering angles. Our result, $r_p = 0.831 \pm 0.007_{\text{stat}} \pm 0.012_{\text{sys}}$ femtometres, is smaller than the most recent high-precision e–p measurement³ and 2.7 standard deviations smaller than the average of all e–p experimental results⁶. The smaller r_p we have now measured supports the value found by two previous muonic hydrogen experiments^{1,7}. In addition, our finding agrees with the revised value (announced in 2019) for the Rydberg constant⁸—one of the most accurately evaluated fundamental constants in physics.

Electromagnetic and Weak form factors

- The study of electromagnetic form factors is crucial to understanding the substructure of hadrons, where a lot of theoretical and experimental efforts have been made.

PRL 112, 132503 (2014)

JLab Measurement of the Elastic Electron-Proton Scattering Cross Section at $Q^2 = 0.045$ GeV 2

A. Camsonne,²² A. T. Katramatou,²² A. Baldwin,¹¹ J.-P. Chen,²² S. Chien,²² S. Frullani,^{8,10} F. Garibaldi,⁸ T. Holmstrom,¹³ J. Huang,¹⁴ M. G. Kumbartzki,¹⁶ B. Lee,¹⁸ J. J. Markowitz,⁴ S. Marrone,⁶ D. A. Puckett,¹⁴ X. Qian,³ O. Rondor,¹⁴ R. R. Subedi,²³ R. Suleiman,²² V. V. Xiong,¹ A. Gasparian,¹ C. Peng,¹ X. Bai,² L. Ye,² K. G. Meazian,² Z. Ye,² K. Adhikari,² C. Carlini,² A. Dour,² D. Dji,² O. Glamazda,¹ M. L. Kabir,¹ A. Liyanage,¹ J. Maxwell,¹ C. Perdrisat,¹ J. Pierce,¹ V. V. Subedi,¹ V. V. Tarasov,¹ and the Jefferson Lab Hall A Collaboration

Received: 17 June 2019
Accepted: 19 September 2019
Published online: 6 November 2019

https://doi.org/10.1038/s41566-019-1721-2

Elastic electron-proton scattering is the two methods traditionally used to determine the proton's magnetic form factor. Despite experimental advances, there is a discrepancy between the results of the experiment at Jefferson Lab and the results established after the discovery of the free method along with the limitations of previous experiments at forward-scattering angles smaller than the most recent measurements. We have now measured the proton's magnetic form factor with a new method using muon scattering at Jefferson Lab. In addition to the results presented in our previous paper (PRL 119, 201901 (2017)), we have now measured the proton's magnetic form factor with a new method using muon scattering at Jefferson Lab. In addition to the results presented in our previous paper (PRL 119, 201901 (2017)), we have now measured the proton's magnetic form factor with a new method using muon scattering at Jefferson Lab.

PRL 105, 242001 (2010) PHYSICAL REVIEW LETTERS week ending 10 DECEMBER 2010

High-Precision Determination of the Electric and Magnetic Form Factors of the Proton

J. C. Bernauer,^{1,*} P. Achenbach,¹ C. Ayerbe Gayoso,¹ R. Böhm,¹ D. Bosnar,² L. Debenjak,³ M. O. Distler,^{1,†} L. Doria,¹ A. Esser,¹ H. Fonvieille,⁴ J. M. Friedrich,⁵ J. Friedrich,¹ M. Gómez Rodríguez de la Paz,¹ M. Makek,² H. Merkel,¹ D. G. Middleton,¹ U. Müller,¹ L. Nungesser,¹ J. Pochodzalla,¹ M. Potokar,³ S. Sánchez Majos,¹ B. S. Schlimme,¹ S. Širca,^{6,3} Th. Walcher,¹ and M. Weinriefer¹

(A1 Collaboration)

¹Institut für Kernphysik, Johannes Gutenberg-Universität Mainz, 55099 Mainz, Germany
²Department of Physics, University of Zagreb, 10002 Zagreb, Croatia
³Jožef Stefan Institute, Ljubljana, Slovenia
⁴LPC-Clermont, Université Blaise Pascal, CNRS/IN2P3, F-63177 Aubière Cedex, France
⁵Physik-Department, Technische Universität München, 85748 Garching, Germany
⁶Department of Physics, University of Ljubljana, Slovenia

(Received 29 July 2010; published 10 December 2010)

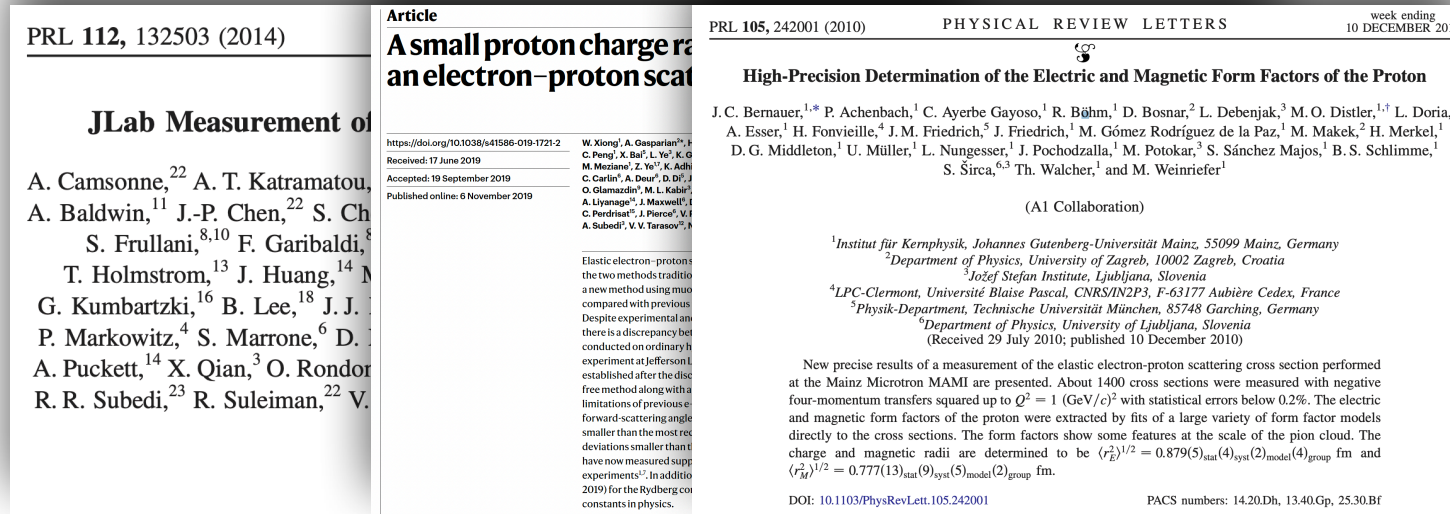
New precise results of a measurement of the elastic electron-proton scattering cross section performed at the Mainz Microtron MAMI are presented. About 1400 cross sections were measured with negative four-momentum transfers squared up to $Q^2 = 1$ (GeV/c) 2 with statistical errors below 0.2%. The electric and magnetic form factors of the proton were extracted by fits of a large variety of form factor models directly to the cross sections. The form factors show some features at the scale of the pion cloud. The charge and magnetic radii are determined to be $\langle r_E^2 \rangle^{1/2} = 0.879(5)_{\text{stat}}(4)_{\text{syst}}(2)_{\text{model}}(4)_{\text{group}}$ fm and $\langle r_M^2 \rangle^{1/2} = 0.777(13)_{\text{stat}}(9)_{\text{syst}}(5)_{\text{model}}(2)_{\text{group}}$ fm.

DOI: 10.1103/PhysRevLett.105.242001

PACS numbers: 14.20.Dh, 13.40.Gp, 25.30.Bf

Electromagnetic and Weak form factors

- The study of electromagnetic form factors is crucial to understanding the substructure of hadrons, where a lot of theoretical and experimental efforts have been made.



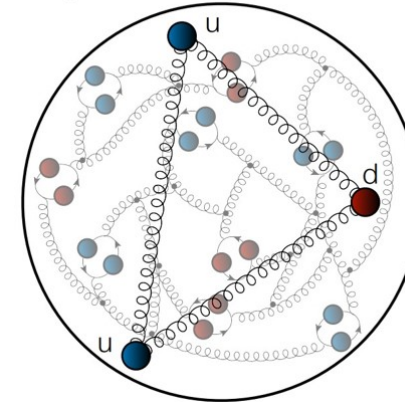
The image shows three overlapping journal article covers. The leftmost cover is from PRL 112, 132503 (2014), titled "JLab Measurement of the Proton Form Factors". The middle cover is from PRL 121, 172501 (2019), titled "A small proton charge radius from an electron-proton scattering experiment". The rightmost cover is from PRL 105, 242001 (2010), titled "High-Precision Determination of the Electric and Magnetic Form Factors of the Proton".

- Weak form factors which included axial and induced pseudoscalar form factors are important quantities for the understanding of weak interactions, neutrino-nucleus scattering and parity violation experiments.

Strong interaction

Proton contains two valence u -quark, one valence d -quark, and infinitely many gluons and sea quarks. These quarks are bound together by the strong interactions, described by quantum chromodynamics (QCD).

A proton

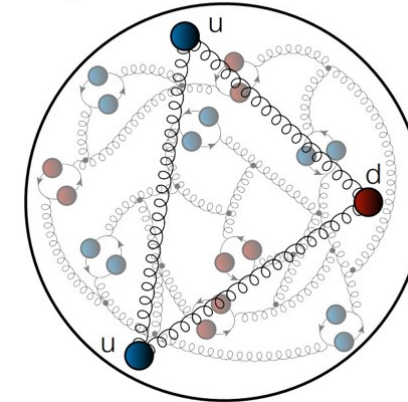


Strong interaction

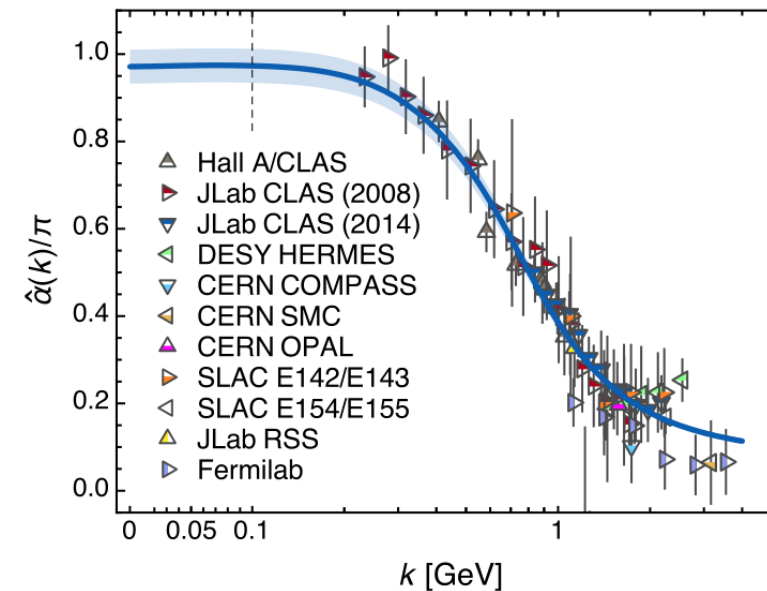
Proton contains two valence u -quark, one valence d -quark, and infinitely many gluons and sea quarks. These quarks are bound together by the strong interactions, described by quantum chromodynamics (QCD).

QCD's Running Coupling is getting large as energy scales decrease.

A proton



Z.-F. Cui *et al* 2020 *Chinese Phys. C* 44 083102



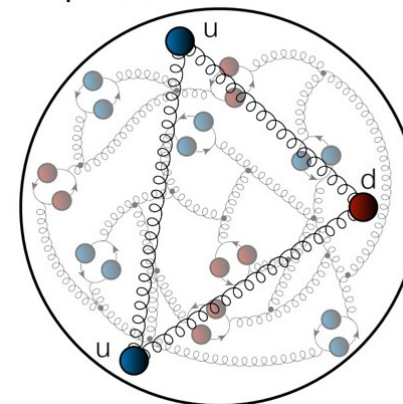
QCD's Running Coupling

Strong interaction

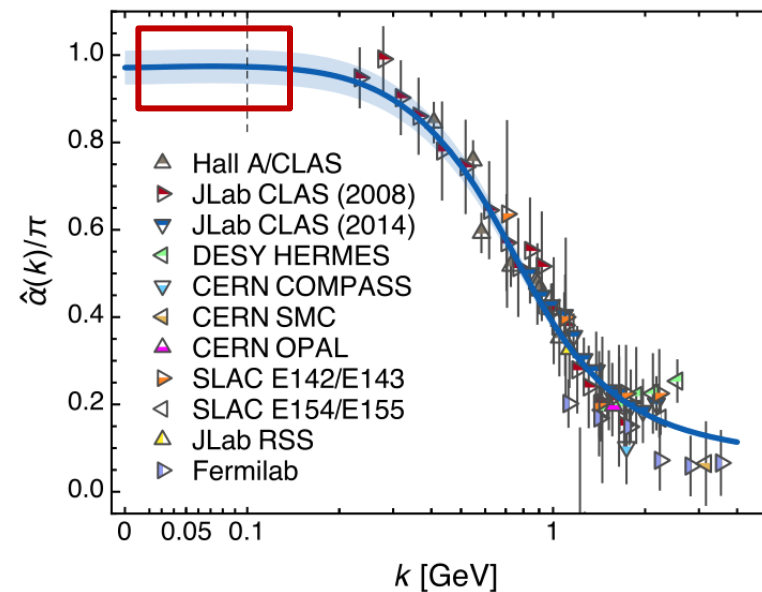
Proton contains two valence u -quark, one valence d -quark, and infinitely many gluons and sea quarks. These quarks are bound together by the strong interactions, described by quantum chromodynamics (QCD).

QCD's Running Coupling is getting large as energy scales decrease.

A proton



Z.-F. Cui *et al* 2020 *Chinese Phys. C* 44 083102

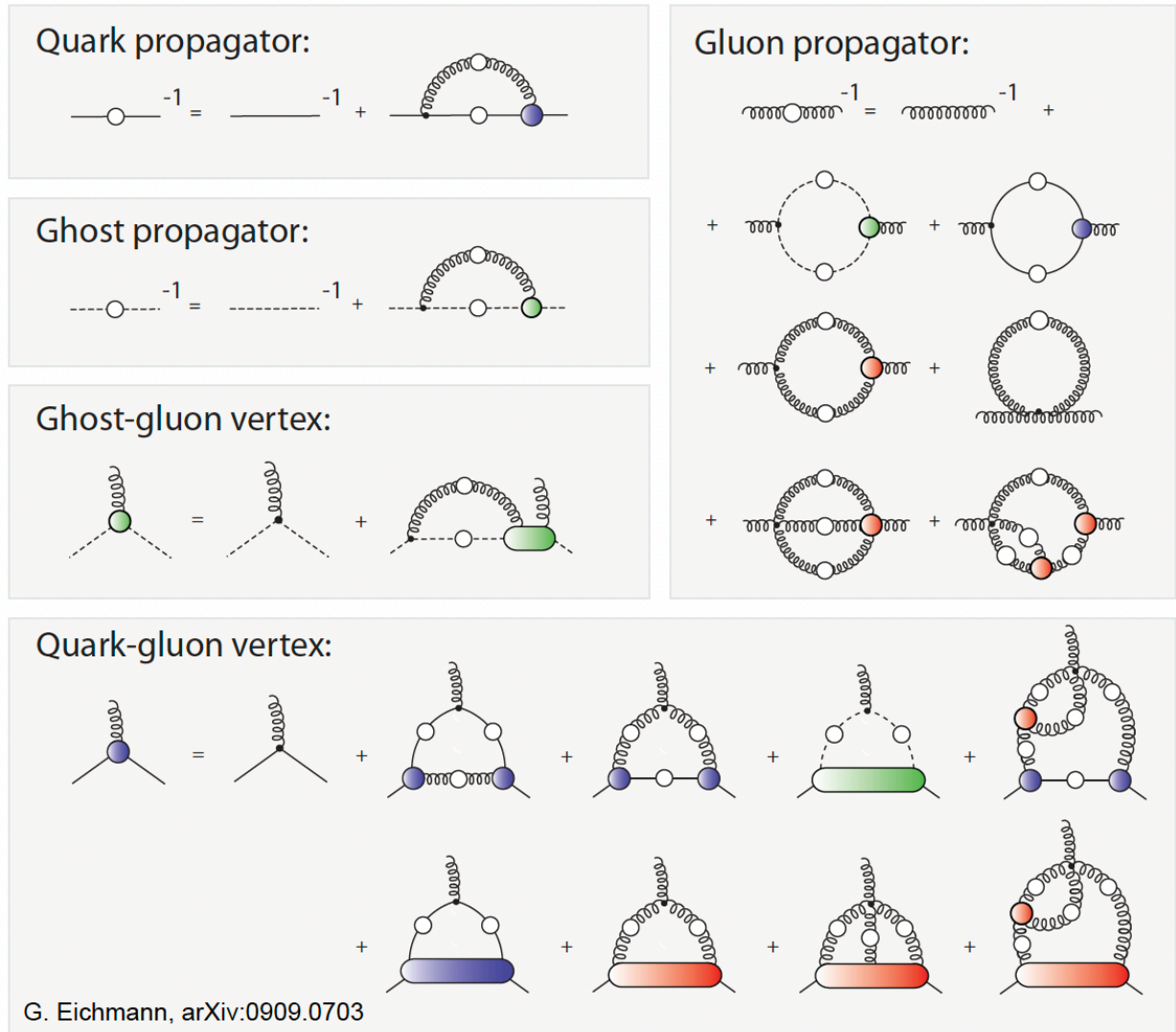


QCD's Running Coupling

Dyson-Schwinger Equations

From the field equations of quantum field theory, one can derive a system of coupled integral equations interrelating all of a theory's Schwinger functions which is the Dyson-Schwinger equations (DSEs).

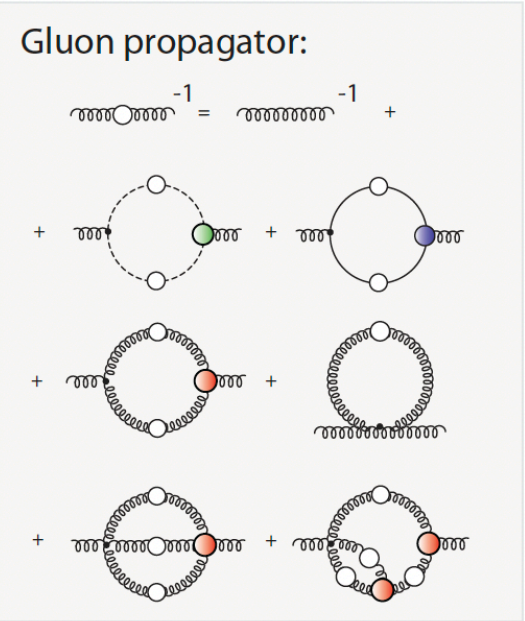
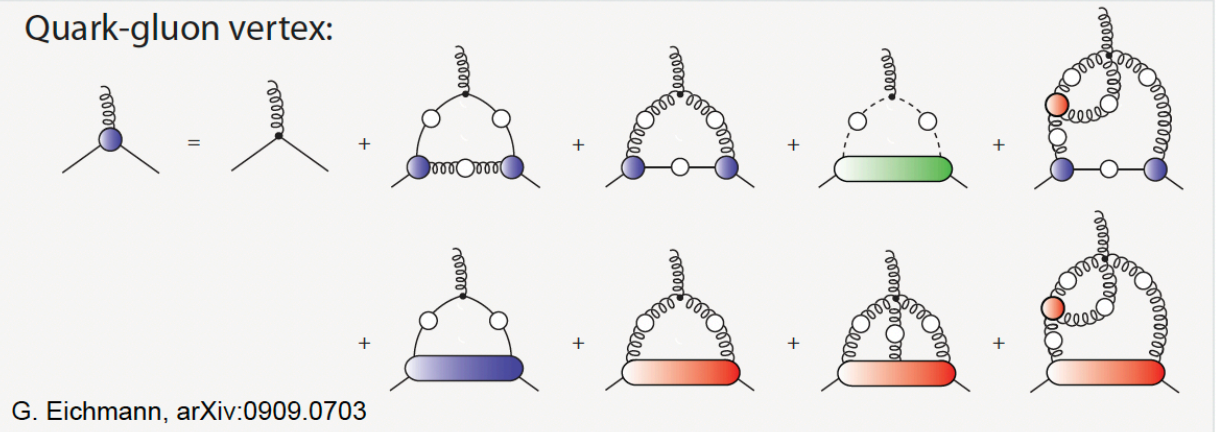
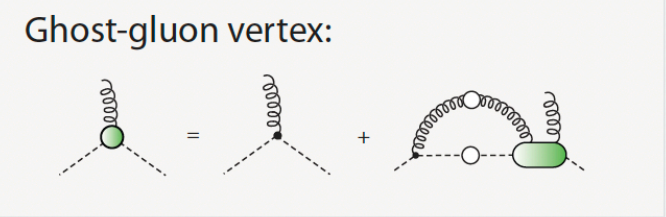
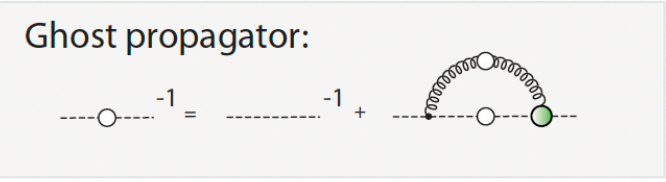
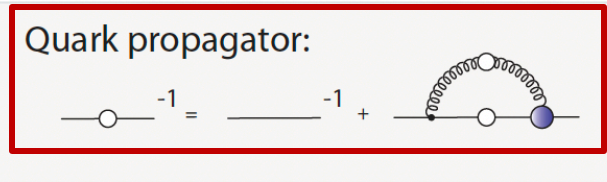
$$G^{(n)}(x_1, \dots, x_n) = \langle \Omega | \phi(x_1) \dots \phi(x_n) | \Omega \rangle$$



Dyson-Schwinger Equations

From the field equations of quantum field theory, one can derive a system of coupled integral equations interrelating all of a theory's Schwinger functions which is the Dyson-Schwinger equations (DSEs).

$$G^{(n)}(x_1, \dots, x_n) = \langle \Omega | \phi(x_1) \dots \phi(x_n) | \Omega \rangle$$



DSE: Gap Equations - one quark

➤ Dressed quark propagator:

$$S(p) = \frac{1}{i\gamma \cdot p A(p^2) + B(p^2)} = \frac{Z(p^2)}{i\gamma \cdot p + M(p^2)}$$

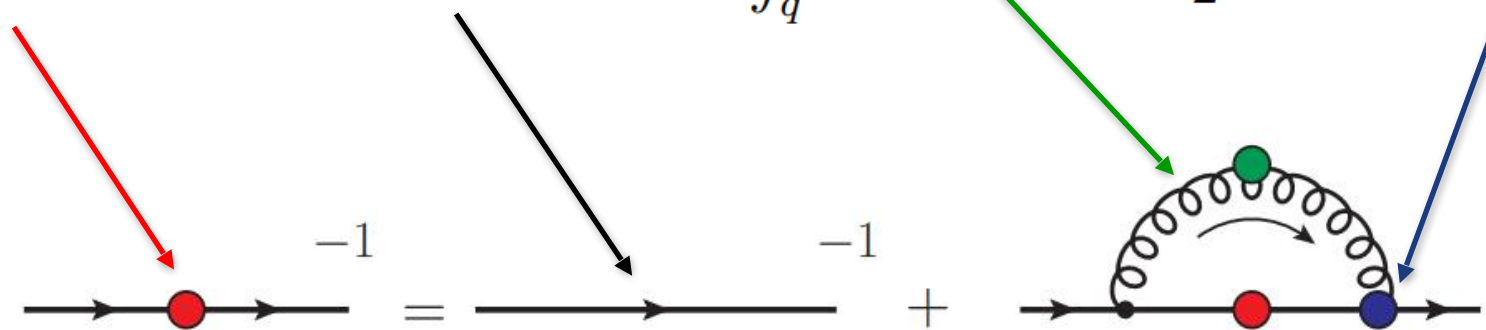
DSE: Gap Equations - one quark

➤ Dressed quark propagator:

$$S(p) = \frac{1}{i\gamma \cdot p A(p^2) + B(p^2)} = \frac{Z(p^2)}{i\gamma \cdot p + M(p^2)}$$

➤ Gap Equation

$$S^{-1}(p) = Z_2(i\gamma \cdot p + m_f^{bm}(\Lambda^2)) + \int_q^\Lambda g^2 D_{\mu\nu}(p-q) \frac{\lambda^a}{2} \gamma_\mu S(q) \Gamma_\nu^a(q,p)$$



DSE: Gap Equations - one quark

➤ Rainbow truncation

$$\Gamma_\nu^a \rightarrow \frac{\lambda^a}{2} \gamma_\nu$$

DSE: Gap Equations - one quark

- Rainbow truncation

$$\Gamma_\nu^a \rightarrow \frac{\lambda^a}{2} \gamma_\nu$$

- Interaction: Qin-Chang Model

$$Z_1 g^2 D_{\mu\nu}(k) \Gamma_\nu(p, q) = Z_2^2 D_{\mu\nu}^{\text{free}}(k) k^2 \mathcal{G}(k^2) \gamma_\nu$$

Si-xue Qin, Lei Chang, Yu-xin Liu, Craig D. Roberts, and David J. Wilson

[Phys. Rev. C **84**, 042202\(R\)](#)

- the free gluon propagator

$$D_{\mu\nu}^{\text{free}}(k) = \frac{1}{k^2} \left(\delta_{\mu\nu} - \frac{k_\mu k_\nu}{k^2} \right)$$

- Qin-Chang Model

$$\mathcal{G}(s) = \frac{8\pi^2}{\omega^4} D e^{-s/\omega^2} + \frac{8\pi^2 \gamma_m \mathcal{F}(s)}{\ln[\tau + (1 + s/\Lambda_{QCD}^2)^2]}$$

$$\mathcal{F}(s) = [1 - e^{-s/(4m_t^2)}] / s$$

- Where $m_t = 0.5 \text{ GeV}$, $\tau = e^2 - 1$, $\Lambda_{QCD} = 0.234 \text{ GeV}$, $\gamma_m = 12/25$.

DSE: Gap Equations - one quark

- Rainbow truncation

$$\Gamma_\nu^a \rightarrow \frac{\lambda^a}{2} \gamma_\nu$$

- Interaction: Qin-Chang Model

$$Z_1 g^2 D_{\mu\nu}(k) \Gamma_\nu(p, q) = Z_2^2 D_{\mu\nu}^{\text{free}}(k) k^2 \mathcal{G}(k^2) \gamma_\nu$$

Si-xue Qin, Lei Chang, Yu-xin Liu, Craig D. Roberts, and David J. Wilson

[Phys. Rev. C **84**, 042202\(R\)](#)

- the free gluon propagator

$$D_{\mu\nu}^{\text{free}}(k) = \frac{1}{k^2} \left(\delta_{\mu\nu} - \frac{k_\mu k_\nu}{k^2} \right)$$

- Qin-Chang Model

$$\mathcal{G}(s) = \frac{8\pi^2}{\omega^4} D e^{-s/\omega^2} + \frac{8\pi^2 \gamma_m \mathcal{F}(s)}{\ln[\tau + (1 + s/\Lambda_{QCD}^2)^2]}$$

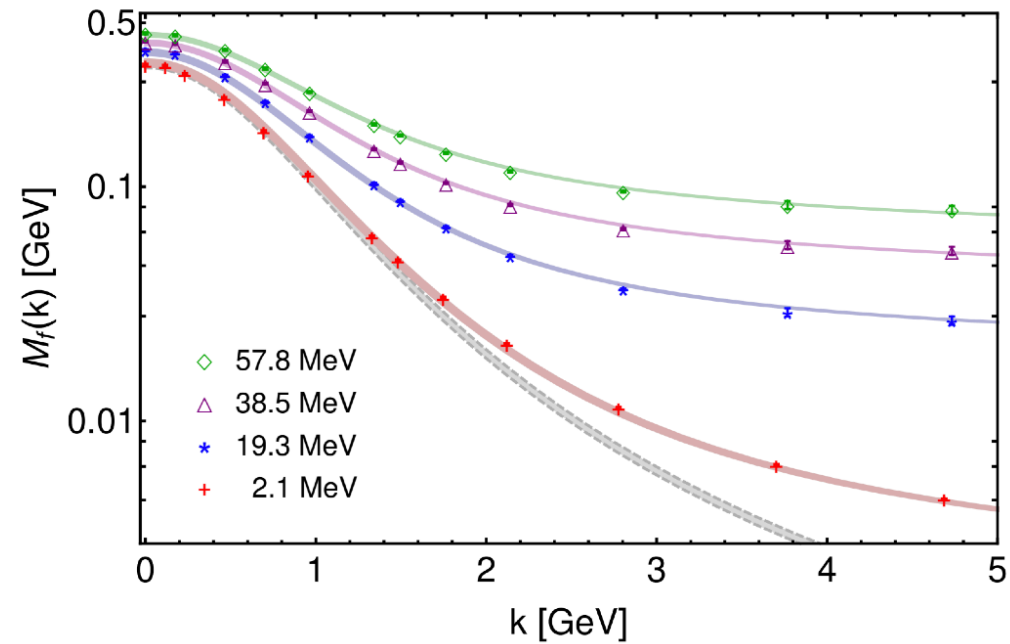
$$\mathcal{F}(s) = [1 - e^{-s/(4m_t^2)}] / s$$

- Where $m_t = 0.5$ GeV, $\tau = e^2 - 1$, $\Lambda_{QCD} = 0.234$ GeV, $\gamma_m = 12/25$.

DSE: Gap Equations - one quark

➤ Dressed quark propagator:

$$S(p) = \frac{1}{i\gamma \cdot p A(p^2) + B(p^2)} = \frac{Z(p^2)}{i\gamma \cdot p + M(p^2)}$$



Chang et. al., PRD 104, 094509 (2021)

DSE: Bethe-Salpeter Equations - two quarks

- Meson: Homogeneous Bethe-Salpeter equation (BSE)

$$\Gamma^{f\bar{g}}(p; P) = Z_2^2 \int_q^\Lambda K(p, q; P) S^f(q_+) \Gamma^{f\bar{g}}(q; P) S^g(q_-)$$

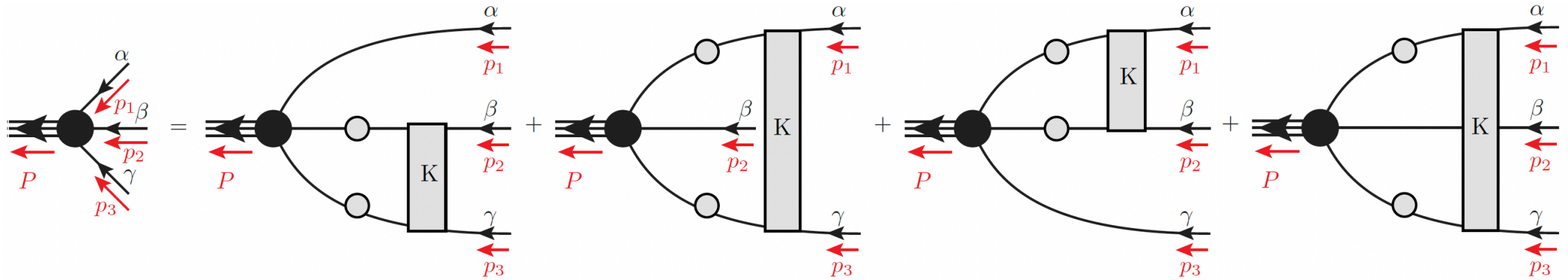
- $P^2 = -m^2$ is total momentum of system, m is the meson mass. (Euclidean space)
- k is relative momentum between valence quark.

- Ladder truncation:

$$K(p, q; P) \rightarrow -\mathcal{G}(k^2) k^2 D_{\mu\nu}^{\text{free}}(k) \frac{\lambda^a}{2} \gamma_\mu \otimes \frac{\lambda^a}{2} \gamma_\nu$$

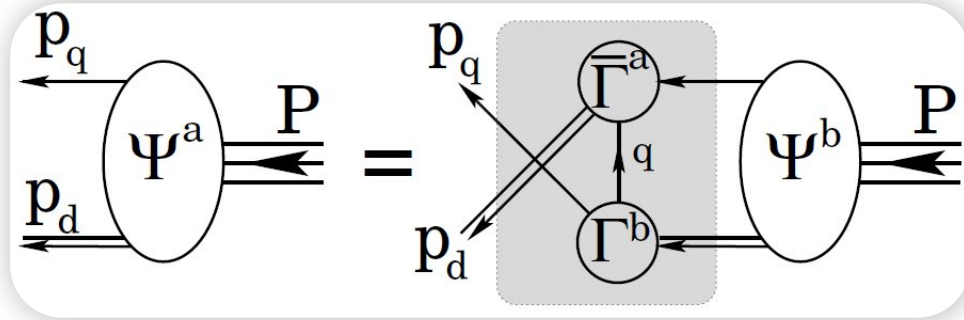
Rainbow-Ladder (RL) truncation is the leading-order in a **nonperturbative, symmetry-preserving** truncation.

DSE: Faddeev equation - three quarks



- Poincaré covariant Faddeev equation sums all possible exchanges and interactions that can take place between three dressed-quarks

DSE: Faddeev equation - three quarks



- Diquark approximation to quark+quark scattering kernel is used for many applications.



Progress in Particle and
Nuclear Physics

Volume 116, January 2021, 103835

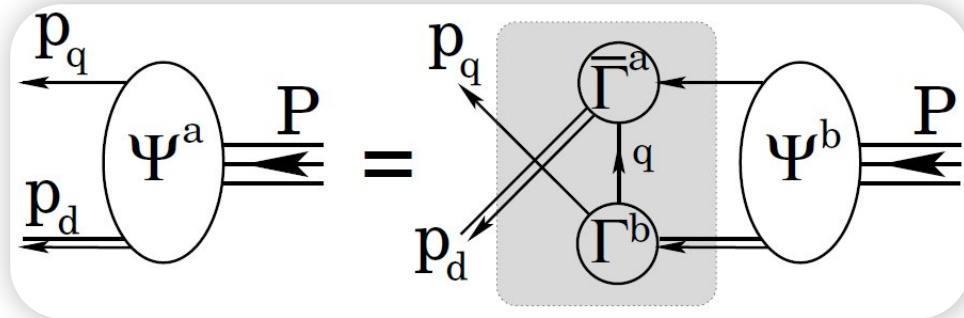


Review

Diquark correlations in hadron physics: Origin, impact and evidence

M.Yu. Barabanov¹, M.A. Bedolla², W.K. Brooks³, G.D. Cates⁴, C. Chen⁵, Y. Chen^{6,7}, E. Cisbani⁸, M. Ding⁹, G. Eichmann^{10,11}, R. Ent¹², J. Ferretti¹³
✉, R.W. Gothe¹⁴, T. Horn^{15,12}, S. Liuti⁴, C. Mezrag¹⁶, A. Pilloni⁹, A.J.R. Puckett¹⁷, C.D. Roberts^{18,19} ✉ ... B.B. Wojtsekhowski¹² ✉

DSE: Faddeev equation - three quarks



- Diquark approximation to quark+quark scattering kernel is used for many applications.
- This motivates the omission of the three-body irreducible contribution from the full three-quark kernel.



Progress in Particle and Nuclear Physics

Volume 116, January 2021, 103835

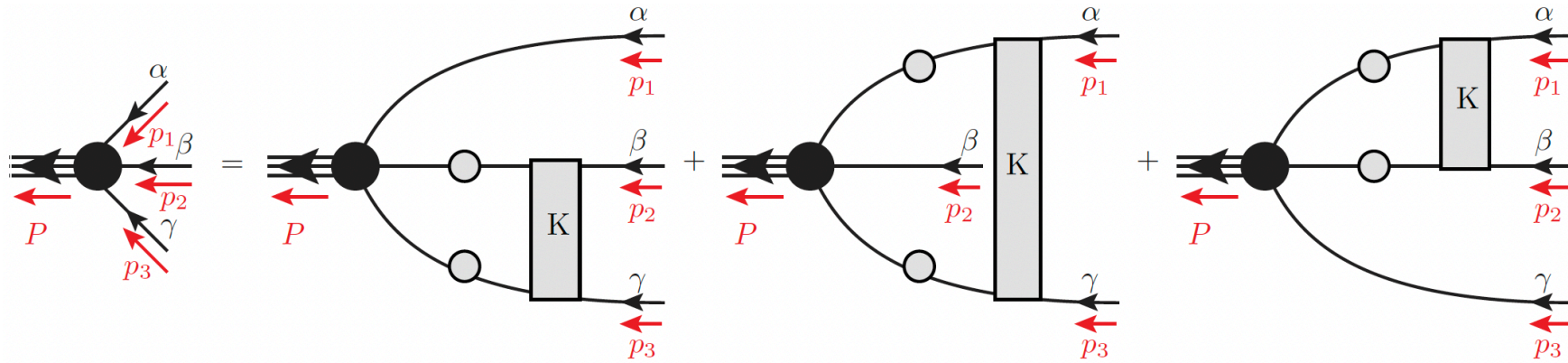


Review

Diquark correlations in hadron physics: Origin, impact and evidence

M.Yu. Barabanov ¹, M.A. Bedolla ², W.K. Brooks ³, G.D. Cates ⁴, C. Chen ⁵, Y. Chen ^{6, 7}, E. Cisbani ⁸, M. Ding ⁹, G. Eichmann ^{10, 11}, R. Ent ¹², J. Ferretti ¹³ ✉, R.W. Gothe ¹⁴, T. Horn ^{15, 12}, S. Liuti ⁴, C. Mezrag ¹⁶, A. Pilloni ⁹, A.J.R. Puckett ¹⁷, C.D. Roberts ^{18, 19} ✉ ... B.B. Wojtsekhowski ¹² ✉

DSE: Faddeev equation - three quarks



$$\Psi_{ABCD}(p, q, P) = \Psi_{ABCD}^{(1)}(p, q, P) + \Psi_{ABCD}^{(2)}(p, q, P) + \Psi_{ABCD}^{(3)}(p, q, P)$$

$$\Psi_{ABCD}^{(1)}(p, q, P) := \int_k K_{BB'CC'}(k) S_{B'B''}(k_2) S_{C'C''}(\tilde{k}_3) \Psi_{AB''C''D}(p^{(1)}, q^{(1)}, P)$$

$$\Psi_{ABCD}^{(2)}(p, q, P) := \int_k K_{CC'AA'}(k) S_{C'C''}(k_3) S_{A'A''}(\tilde{k}_1) \Psi_{A''BC''D}(p^{(2)}, q^{(2)}, P)$$

$$\Psi_{ABCD}^{(3)}(p, q, P) := \int_k K_{AA'BB'}(k) S_{A'A''}(k_1) S_{B'B''}(\tilde{k}_2) \Psi_{A''B''CD}(p^{(3)}, q^{(3)}, P)$$

$$p = (1 - \zeta)p_3 - \zeta(p_1 + p_2);$$

$$q = \frac{p_2 - p_1}{2};$$

$$P = p_1 + p_2 + p_3;$$

$P^2 = -m^2$ is total momentum of 3-quark system, m is the baryon mass.

3-quark Faddeev equation

$$\Psi_{ABCD}^{(3)}(p, q, P) := \int_k K_{AA'BB'}(k) S_{A'A''}(k_1) S_{B'B''}(\tilde{k}_2) \Psi_{A''B''CD}(p^{(3)}, q^{(3)}, P)$$

➤ Amplitude:

$$\Psi_{ABCD}(p, q, P) = \left(\sum_{\rho} \psi_{\alpha\beta\gamma\mathcal{I}}^{\rho}(p, q, P) \otimes F_{abcd}^{\rho} \right) \otimes \frac{\epsilon_{rst}}{\sqrt{6}}$$

3-quark Faddeev equation

$$\Psi_{ABCD}^{(3)}(p, q, P) := \int_k K_{AA'BB'}(k) S_{A'A''}(k_1) S_{B'B''}(\tilde{k}_2) \Psi_{A''B''CD}(p^{(3)}, q^{(3)}, P)$$

➤ Amplitude:

$$\Psi_{ABCD}(p, q, P) = \left(\sum_{\rho} \psi_{\alpha\beta\gamma\mathcal{I}}^{\rho}(p, q, P) \otimes F_{abcd}^{\rho} \right) \otimes \frac{\epsilon_{rst}}{\sqrt{6}}$$

1. the color term fixes the baryon to be a color singlet;

3-quark Faddeev equation

$$\Psi_{ABCD}^{(3)}(p, q, P) := \int_k K_{AA'BB'}(k) S_{A'A''}(k_1) S_{B'B''}(\tilde{k}_2) \Psi_{A''B''CD}(p^{(3)}, q^{(3)}, P)$$

➤ Amplitude:

$$\Psi_{ABCD}(p, q, P) = \left(\sum_{\rho} \psi_{\alpha\beta\gamma\mathcal{I}}^{\rho}(p, q, P) \otimes \mathbf{F}_{abcd}^{\rho} \right) \otimes \frac{\epsilon_{rst}}{\sqrt{6}}.$$

1. the color term fixes the baryon to be a color singlet;
2. flavor amplitudes are the quark model SU(3) representation;

state	$F_{\mathcal{M}_A}$	$F_{\mathcal{M}_S}$
p	$\frac{1}{\sqrt{2}}(udu - duu)$	$\frac{1}{\sqrt{6}}(2ud - udu - duu)$
n	$\frac{1}{\sqrt{2}}(udd - dud)$	$\frac{1}{\sqrt{6}}(udd + dud - 2ddu)$
Σ^+	$\frac{1}{\sqrt{2}}(usu - suu)$	$\frac{1}{\sqrt{6}}(2uus - usu - suu)$
Σ^0	$\frac{1}{2}(usd + dsu - sud - sdu)$	$\frac{1}{\sqrt{12}}(2uds + 2dus - usd - dsu - sud - sdu)$
Σ^-	$\frac{1}{\sqrt{2}}(dsd - sdd)$	$\frac{1}{\sqrt{6}}(2dds - dsd - sdd)$
Ξ^0	$\frac{1}{\sqrt{2}}(uss - sus)$	$\frac{1}{\sqrt{6}}(uss + sus - 2ssu)$
Ξ^-	$\frac{1}{\sqrt{2}}(dss - sds)$	$\frac{1}{\sqrt{6}}(dss + sds - 2ssd)$
Λ^0	$\frac{1}{\sqrt{12}}(2uds - 2dus + sdu - dsu + usd - sud)$	$\frac{1}{2}(usd + sud - dsu - sdu)$

Table 1: Baryon octet flavor amplitudes; we define $\lambda_1 \lambda_2 \lambda_3 := \lambda_1 \otimes \lambda_2 \otimes \lambda_3$, and, $u^\dagger := (1 \ 0 \ 0)$, $d^\dagger := (0 \ 1 \ 0)$, $s^\dagger := (0 \ 0 \ 1)$.

3-quark Faddeev equation

$$\Psi_{ABCD}^{(3)}(p, q, P) := \int_k K_{AA'BB'}(k) S_{A'A''}(k_1) S_{B'B''}(\tilde{k}_2) \Psi_{A''B''CD}(p^{(3)}, q^{(3)}, P)$$

➤ Amplitude:

$$\Psi_{ABCD}(p, q, P) = \left(\sum_{\rho} \psi_{\alpha\beta\gamma\mathcal{I}}^{\rho}(p, q, P) \otimes F_{abcd}^{\rho} \right) \otimes \frac{\epsilon_{rst}}{\sqrt{6}}.$$

1. the color term fixes the baryon to be a color singlet;
2. flavor amplitudes are the quark model SU(3) representation;
3. spin-momentum Faddeev amplitude.

state	$F_{\mathcal{M}_A}$	$F_{\mathcal{M}_S}$
p	$\frac{1}{\sqrt{2}}(udu - duu)$	$\frac{1}{\sqrt{6}}(2uud - udu - duu)$
n	$\frac{1}{\sqrt{2}}(udd - dud)$	$\frac{1}{\sqrt{6}}(udd + dud - 2ddu)$
Σ^+	$\frac{1}{\sqrt{2}}(usu - suu)$	$\frac{1}{\sqrt{6}}(2uus - usu - suu)$
Σ^0	$\frac{1}{2}(usd + dsu - sud - sdu)$	$\frac{1}{\sqrt{12}}(2uds + 2dus - usd - dsu - sud - sdu)$
Σ^-	$\frac{1}{\sqrt{2}}(dsd - sdd)$	$\frac{1}{\sqrt{6}}(2dds - dsd - sdd)$
Ξ^0	$\frac{1}{\sqrt{2}}(uss - sus)$	$\frac{1}{\sqrt{6}}(uss + sus - 2ssu)$
Ξ^-	$\frac{1}{\sqrt{2}}(dss - sds)$	$\frac{1}{\sqrt{6}}(dss + sds - 2ssd)$
Λ^0	$\frac{1}{\sqrt{12}}(2uds - 2dus + sdu - dsu + usd - sud)$	$\frac{1}{2}(usd + sud - dsu - sdu)$

Table 1: Baryon octet flavor amplitudes; we define $\lambda_1\lambda_2\lambda_3 := \lambda_1 \otimes \lambda_2 \otimes \lambda_3$, and, $u^\dagger := (1\ 0\ 0)$, $d^\dagger := (0\ 1\ 0)$, $s^\dagger := (0\ 0\ 1)$.

3-quark Faddeev equation

$$\Psi_{ABCD}^{(3)}(p, q, P) := \int_k \boxed{K_{AA'BB'}(k)} S_{A'A''}(k_1) S_{B'B''}(\tilde{k}_2) \Psi_{A''B''CD}(p^{(3)}, q^{(3)}, P)$$

➤ Ladder truncation:

$$K_{AA'BB'}(k) = K_{\alpha\alpha'\beta\beta'}(k) k_{aa'}^F k_{bb'},$$

$$K(k) \rightarrow -\mathcal{G}(k^2) k^2 D_{\mu\nu}^{\text{free}}(k) \frac{\lambda^a}{2} \gamma_\mu \otimes \frac{\lambda^a}{2} \gamma_\nu$$

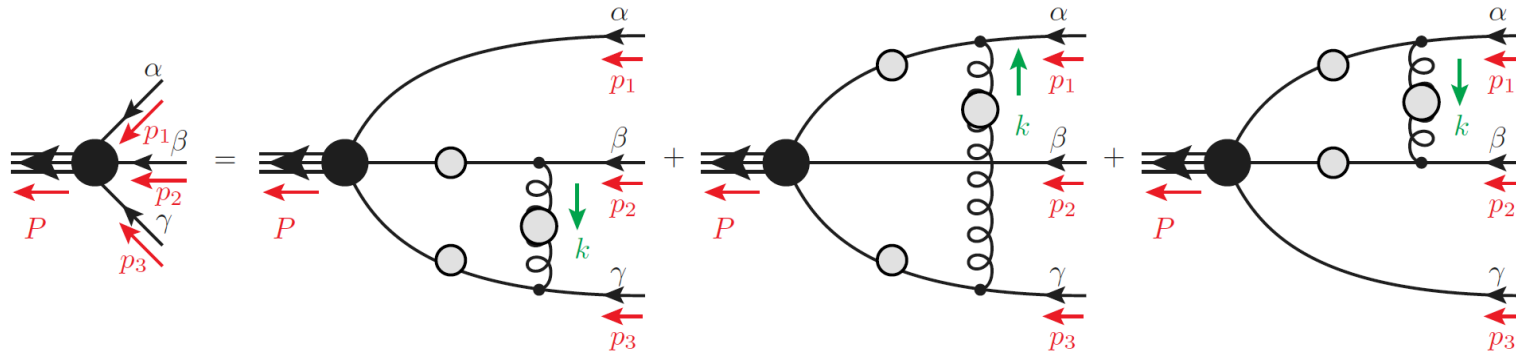
3-quark Faddeev equation

$$\Psi_{ABCD}^{(3)}(p, q, P) := \int_k \boxed{K_{AA'BB'}(k)} S_{A'A''}(k_1) S_{B'B''}(\tilde{k}_2) \Psi_{A''B''CD}(p^{(3)}, q^{(3)}, P)$$

➤ Ladder truncation:

$$K_{AA'BB'}(k) = K_{\alpha\alpha'\beta\beta'}(k) k_{aa'bb'}^F,$$

$$K(k) \rightarrow -\mathcal{G}(k^2) k^2 D_{\mu\nu}^{\text{free}}(k) \frac{\lambda^a}{2} \gamma_\mu \otimes \frac{\lambda^a}{2} \gamma_\nu$$



3-quark Faddeev equation

➤ spin-momentum Faddeev amplitude:

$$\psi_{\alpha\beta\gamma\mathcal{I}}(p, q, P) := \sum_i f_i(p^2, q^2, z_0, z_1, z_2) X_{i,\alpha\beta\gamma\mathcal{I}}(p, q, P),$$

$$p^2; \quad q^2; \quad z_0 = \widehat{p}_T \cdot \widehat{q}_T; \quad z_1 = \widehat{p} \cdot \widehat{P}; \quad z_2 = \widehat{q} \cdot \widehat{P},$$

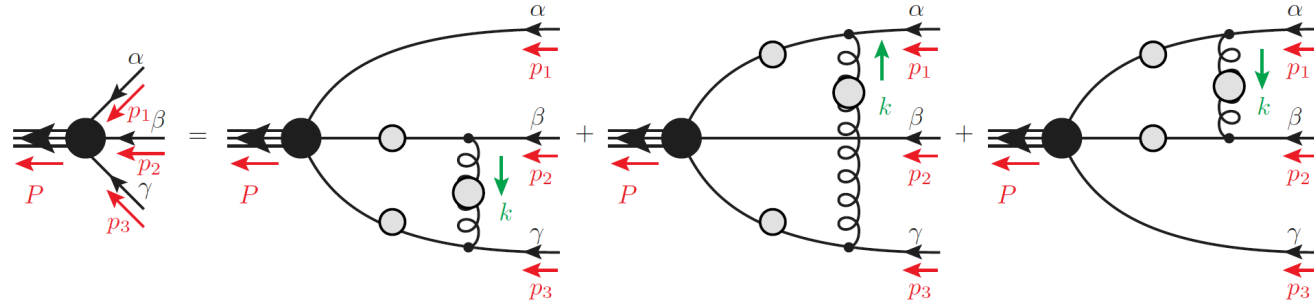
For octet baryons, they have 64 bases and 128 coefficients.

3-quark Faddeev equation

➤ spin-momentum Faddeev amplitude:

$$\psi_{\alpha\beta\gamma\mathcal{I}}(p, q, P) := \sum_i f_i(p^2, q^2, \mathbf{0}, z_1, z_2) X_{i,\alpha\beta\gamma\mathcal{I}}(p, q, P),$$

$$p^2; \quad q^2; \quad z_0 = \mathbf{0}; \quad z_1 = \hat{p} \cdot \hat{P}; \quad z_2 = \hat{q} \cdot \hat{P},$$



PRL **104**, 201601 (2010)

PHYSICAL REVIEW LETTERS

week ending
21 MAY 2010

Nucleon Mass from a Covariant Three-Quark Faddeev Equation

G. Eichmann,^{1,2} R. Alkofer,² A. Krassnigg,² and D. Nicorus²

¹*Institute for Nuclear Physics, Darmstadt University of Technology, 64289 Darmstadt, Germany*

²*Institut für Physik, Karl-Franzens-Universität Graz, 8010 Graz, Austria*

(Received 14 December 2009; published 21 May 2010)

We report the first study of the nucleon where the full Poincaré-covariant structure of the three-quark amplitude is implemented in the Faddeev equation. We employ an interaction kernel which is consistent with contemporary studies of meson properties and aspects of chiral symmetry and its dynamical breaking, thus yielding a comprehensive approach to hadron physics. The resulting current-mass evolution of the nucleon mass compares well with lattice data and deviates only by $\sim 5\%$ from the quark-diquark result obtained in previous studies.

DOI: [10.1103/PhysRevLett.104.201601](https://doi.org/10.1103/PhysRevLett.104.201601)

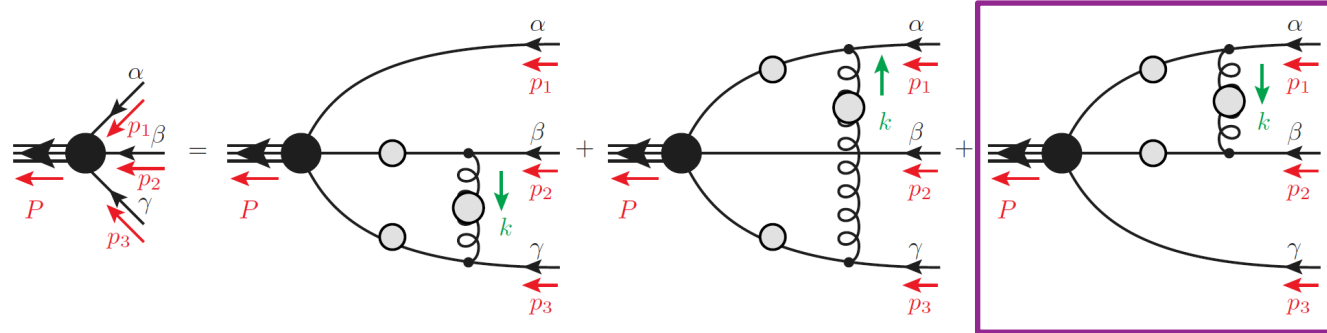
PACS numbers: 11.10.St, 12.38.Lg, 14.20.Dh

3-quark Faddeev equation

➤ spin-momentum Faddeev amplitude:

$$\psi_{\alpha\beta\gamma\mathcal{I}}(p, q, P) := \sum_i f_i(p^2, q^2, z_0, z_1, z_2) X_{i,\alpha\beta\gamma\mathcal{I}}(p, q, P),$$

$$p^2; \quad q^2; \quad z_0 = \widehat{p}_T \cdot \widehat{q}_T; \quad z_1 = \widehat{p} \cdot \widehat{P}; \quad z_2 = \widehat{q} \cdot \widehat{P},$$



PHYSICAL REVIEW D **97**, 114017 (2018)

PHYSICAL REVIEW D **84**, 014014 (2011)

Nucleon electromagnetic form factors from the covariant Faddeev equation

G. Eichmann*

Institut für Theoretische Physik I, Justus-Liebig-Universität Giessen, D-35392 Giessen, Germany

(Received 28 April 2011; published 11 July 2011)

We compute the electromagnetic form factors of the nucleon in the Poincaré-covariant Faddeev framework based on the Dyson-Schwinger equations of QCD. The general expression for a baryon's electromagnetic current in terms of three interacting dressed quarks is derived. Upon employing a rainbow-ladder gluon-exchange kernel for the quark-quark interaction, the nucleon's Faddeev amplitude and electromagnetic form factors are computed without any further truncations or model assumptions. The form-factor results show clear evidence of missing pion-cloud effects below a photon momentum transfer of $\sim 2 \text{ GeV}^2$ and in the chiral region, whereas they agree well with experimental data at higher photon momenta. Thus, the approach reflects the properties of the nucleon's quark core.

DOI: 10.1103/PhysRevD.84.014014

PACS numbers: 12.38.Lg, 11.80.Jy, 13.40.Gp, 14.20.Dh

Poincaré-covariant analysis of heavy-quark baryons

Si-Xue Qin,^{1,*} Craig D. Roberts,^{2,†} and Sebastian M. Schmidt^{3,‡}

¹Department of Physics, Chongqing University, Chongqing 401331, People's Republic of China

²Physics Division, Argonne National Laboratory, Argonne, Illinois 60439, USA

³Institute for Advanced Simulation, Forschungszentrum Jülich and JARA, D-52425 Jülich, Germany

(Received 29 January 2018; published 13 June 2018)

We use a symmetry-preserving truncation of meson and baryon bound-state equations in quantum field theory in order to develop a unified description of systems constituted from light and heavy quarks. In particular, we compute the spectrum and leptonic decay constants of ground-state pseudoscalar and vector mesons: $q'\bar{q}$, $Q'\bar{Q}$, with $q', q = u, d, s$ and $Q', Q = c, b$, and the masses of $J^P = 3/2^+$ baryons and their first positive-parity excitations, including those containing one or more heavy quarks. This Poincaré-covariant analysis predicts that such baryons have a complicated angular momentum structure. For instance, the ground states are all primarily S wave in character, but each possesses P -, D - and F -wave components, with the P -wave fraction being large in the qqq states, and the first positive-parity excitation in each channel having a large D -wave component, which grows with increasing current-quark mass, but also exhibits features consistent with a radial excitation. The configuration space extent of all such baryons decreases as the mass of the valence-quark constituents increases.

DOI: 10.1103/PhysRevD.97.114017

3-quark Faddeev equation

- spin-momentum Faddeev amplitude:

$$\psi_{\alpha\beta\gamma\mathcal{I}}(p, q, P) := \sum_i f_i(p^2, q^2, z_0, z_1, z_2) X_{i,\alpha\beta\gamma\mathcal{I}}(p, q, P),$$

$$p^2; \quad q^2; \quad z_0 = \widehat{p}_T \cdot \widehat{q}_T; \quad z_1 = \widehat{p} \cdot \widehat{P}; \quad z_2 = \widehat{q} \cdot \widehat{P},$$

- After making algorithmic improvement and overcoming numerical problems,
direct calculation of Faddeev equation using rainbow-ladder truncation is now possible.

3-quark Faddeev equation

➤ spin-momentum Faddeev amplitude:

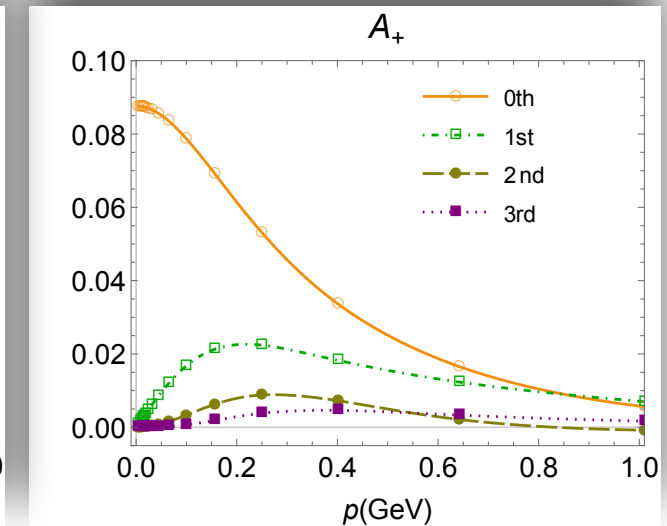
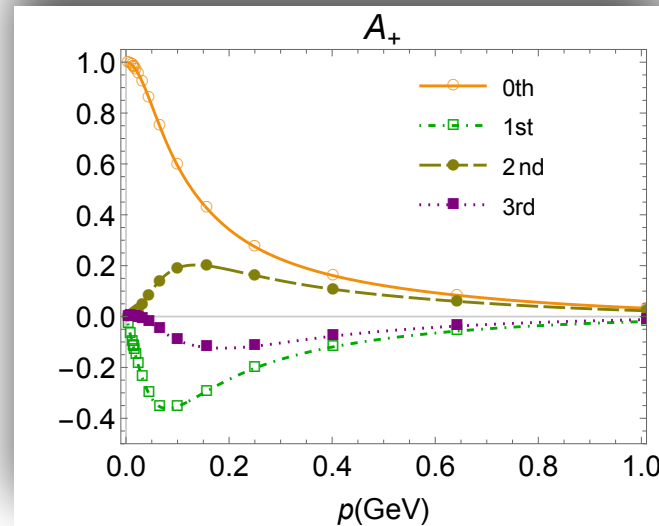
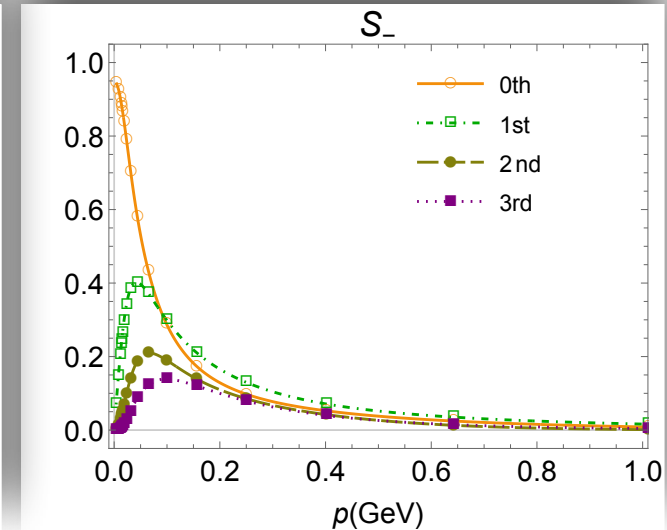
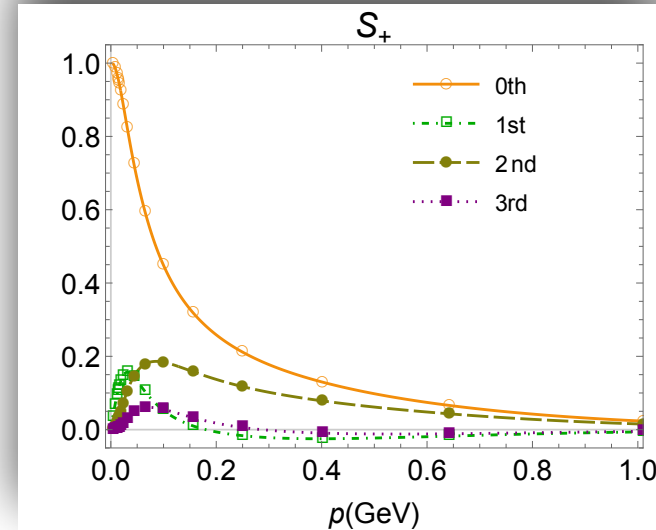
$$\psi_{\alpha\beta\gamma\mathcal{I}}(p, q, P) := \sum_i f_i(p^2, q^2, z_0, z_1, z_2) X_{i,\alpha\beta\gamma\mathcal{I}}(p, q, P),$$

$$p^2; \quad q^2; \quad z_0 = \widehat{p}_T \cdot \widehat{q}_T; \quad z_1 = \widehat{p} \cdot \widehat{P}; \quad z_2 = \widehat{q} \cdot \widehat{P},$$

➤ After making algorithmic improvement and overcoming numerical problems, **direct calculation of Faddeev equation using rainbow-ladder truncation is now possible.**

$$\psi_{\mathcal{M}_S} : \quad \mathcal{S}_{\pm} := \Lambda_{\pm} \gamma_5 C \otimes \Lambda_{+};$$

$$\psi_{\mathcal{M}_A} : \quad \mathcal{A}_{\pm} := \frac{1}{\sqrt{3}} \gamma_5 \gamma_T^{\alpha} \Lambda_{\pm} \gamma_5 C \otimes \gamma_5 \gamma_T^{\alpha} \Lambda_{+},$$



First four Chebyshev moments in the variable z_1 of the dressing functions evaluated at $q = 0$.

3-quark Faddeev equation

- spin-momentum Faddeev amplitude:

$$\psi_{\alpha\beta\gamma\mathcal{I}}(p, q, P) := \sum_i f_i(p^2, q^2, z_0, z_1, z_2) X_{i,\alpha\beta\gamma\mathcal{I}}(p, q, P),$$

$$p^2; \quad q^2; \quad z_0 = \widehat{p}_T \cdot \widehat{q}_T; \quad z_1 = \widehat{p} \cdot \widehat{P}; \quad z_2 = \widehat{q} \cdot \widehat{P},$$

- After making algorithmic improvement and overcoming numerical problems, **direct calculation of Faddeev equation using rainbow-ladder truncation is now possible.**

Table 3: Computed masses of $J = 1/2$ baryons. The interaction scale are $\omega = 0.8$ GeV and $D = 1.0$. The current-quark masses which are $m_u^{\zeta^{19}} = 3.21$ MeV and $m_s^{\zeta^{19}} = 77.5$ MeV. These are chosen to reproduce the empirical values of $m_\pi = 0.14$ GeV, $m_K = 0.50$ GeV, and $f_\pi = 0.094$ GeV; $f_K = 0.11$ GeV. (All quantities listed in GeV; and experimental values drawn from Ref. [40].)

	N	$\Lambda(uds)$	$\Sigma(uus)$	$\Xi(uss)$
Herein	0.938	1.071	1.115	1.333
E [13]&S [31]	0.94	1.073(1)	1.073 (1)	1.235(5)
expt. or lQCD	0.94	1.116	1.189	1.315

Electromagnetic form factors

- The nucleon matrix elements of the electromagnetic current is parametrized by the Dirac form factor F_1 and Pauli form factors F_2 :

$$\begin{aligned} J_E^{\mu B}(P, Q) &:= \left\langle B(p_f) \left| V^{\mu}(Q) \right| B(p_i) \right\rangle \\ &= i\Lambda_+(p_f)(F_1^B(Q^2)\gamma^{\mu} - \frac{F_2^B(Q^2)}{2M_B}\sigma^{\mu\nu}Q^{\nu})\Lambda_+(p_i) \end{aligned}$$

Electromagnetic form factors

- The nucleon matrix elements of the electromagnetic current is parametrized by the Dirac form factor F_1 and Pauli form factors F_2 :

$$\begin{aligned} J_E^\mu{}^B(P, Q) &:= \left\langle B(p_f) \left| V^\mu(Q) \right| B(p_i) \right\rangle \\ &= i\Lambda_+(p_f)(F_1^B(Q^2)\gamma^\mu - \frac{F_2^B(Q^2)}{2M_B}\sigma^{\mu\nu}Q^\nu)\Lambda_+(p_i) \end{aligned}$$

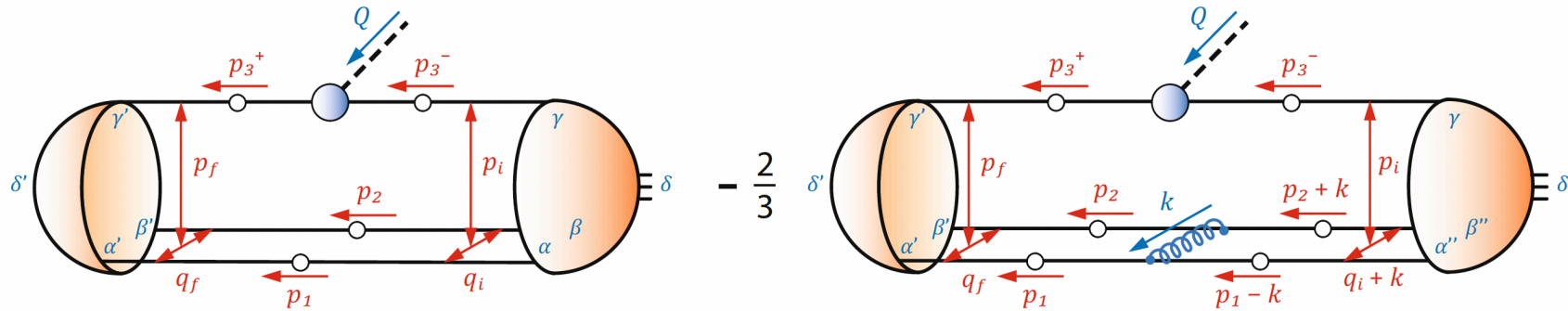
- Sachs form factors:

$$G_E^B = F_1^B - \tau F_2^B; \quad G_M^B = F_1^B + F_2^B,$$

with $\tau = Q^2/(4M_B^2)$.

Electromagnetic form factors

➤ Impulse-approximation diagram baryons' current:

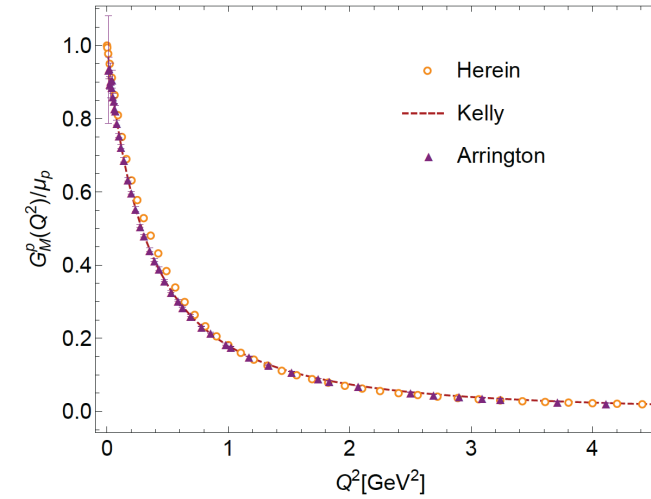
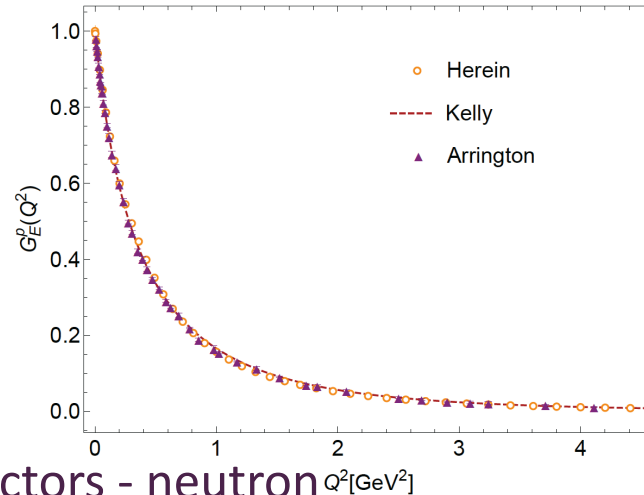


➤ The electromagnetic current:

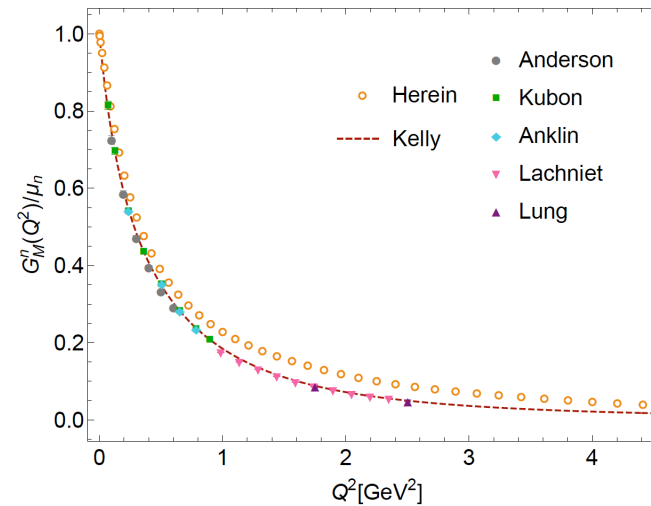
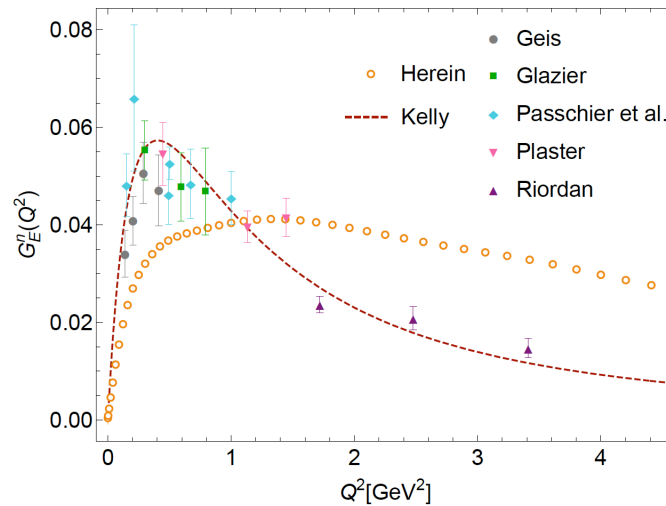
$$\begin{aligned}
 [J_E^{(3)}]_{\delta'\delta} &= \iint_{pq} \bar{\Psi}_{\beta'\alpha'\delta'\gamma'}(p_f, q_f, P_f) S_{\alpha'\alpha}(p_1) S_{\beta'\beta}(p_2) \\
 &\times \left[S(p_3^+) \Gamma_5^{(\mu)}(p_3^+, p_3^-) S(p_3^-) \right]_{\gamma'\gamma} \left[\Psi_{\alpha\beta\gamma\delta}(p_i, q_i, P_i) - \frac{2}{3} \Psi_{\alpha\beta\gamma\delta}^{(3)}(p_i, q_i, P_i) \right]
 \end{aligned}$$

Electromagnetic form factors - proton&neutron

➤ Electromagnetic form factors - proton



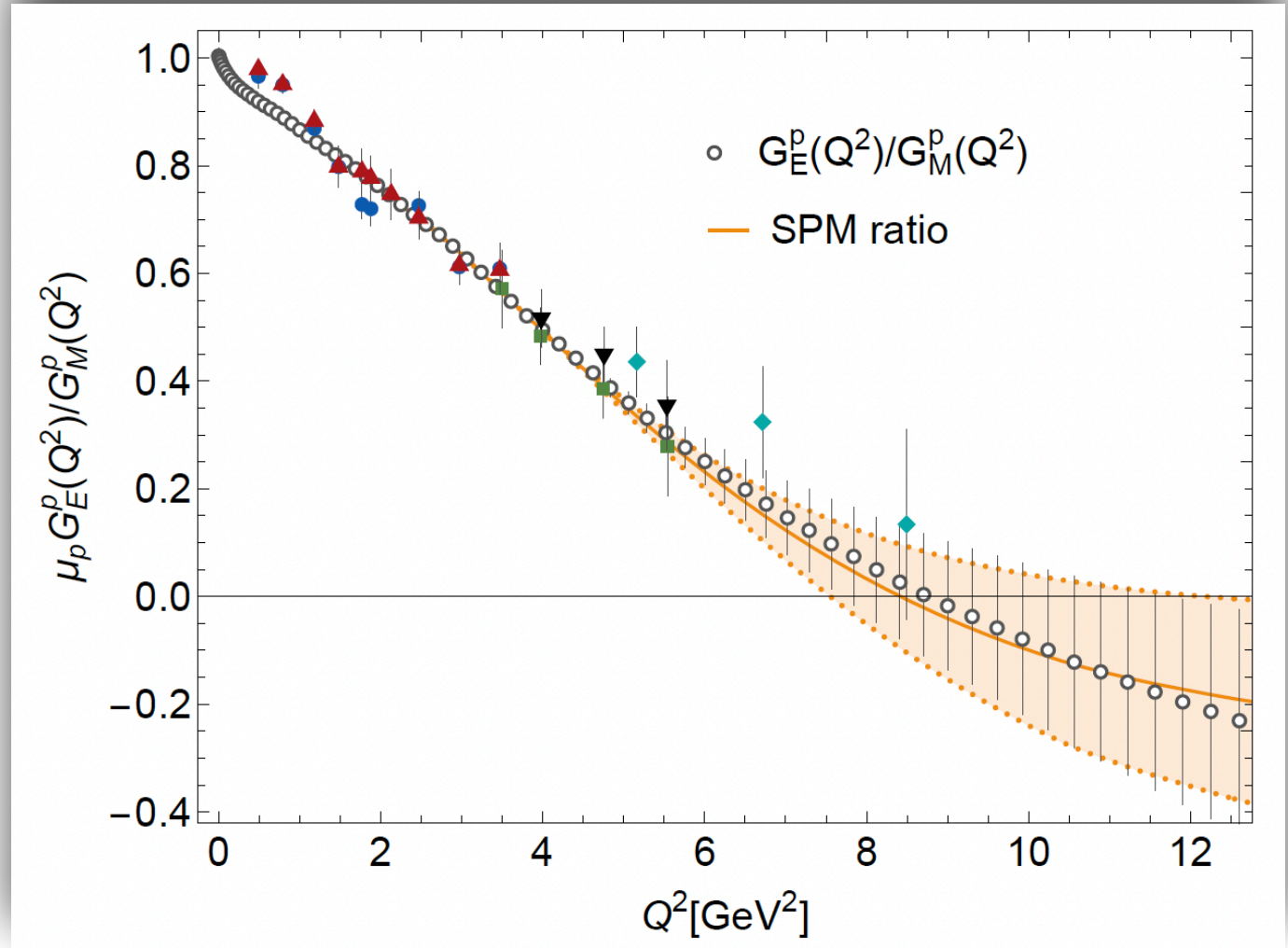
➤ Electromagnetic form factors - neutron



Electromagnetic form factors at large Q^2

- Schlessinger point method (SPM) has been used for study the form factor at large Q^2 .
- Data at JLab show a trend toward zero with increasing momentum transfer.
- Ratio for proton:

$$\frac{\mu_p G_E^p}{G_M^p} = 0 \text{ at } Q^2 = 8.42^{+3.76}_{-0.86} \text{ GeV}^2$$



Electromagnetic form factors at large Q^2

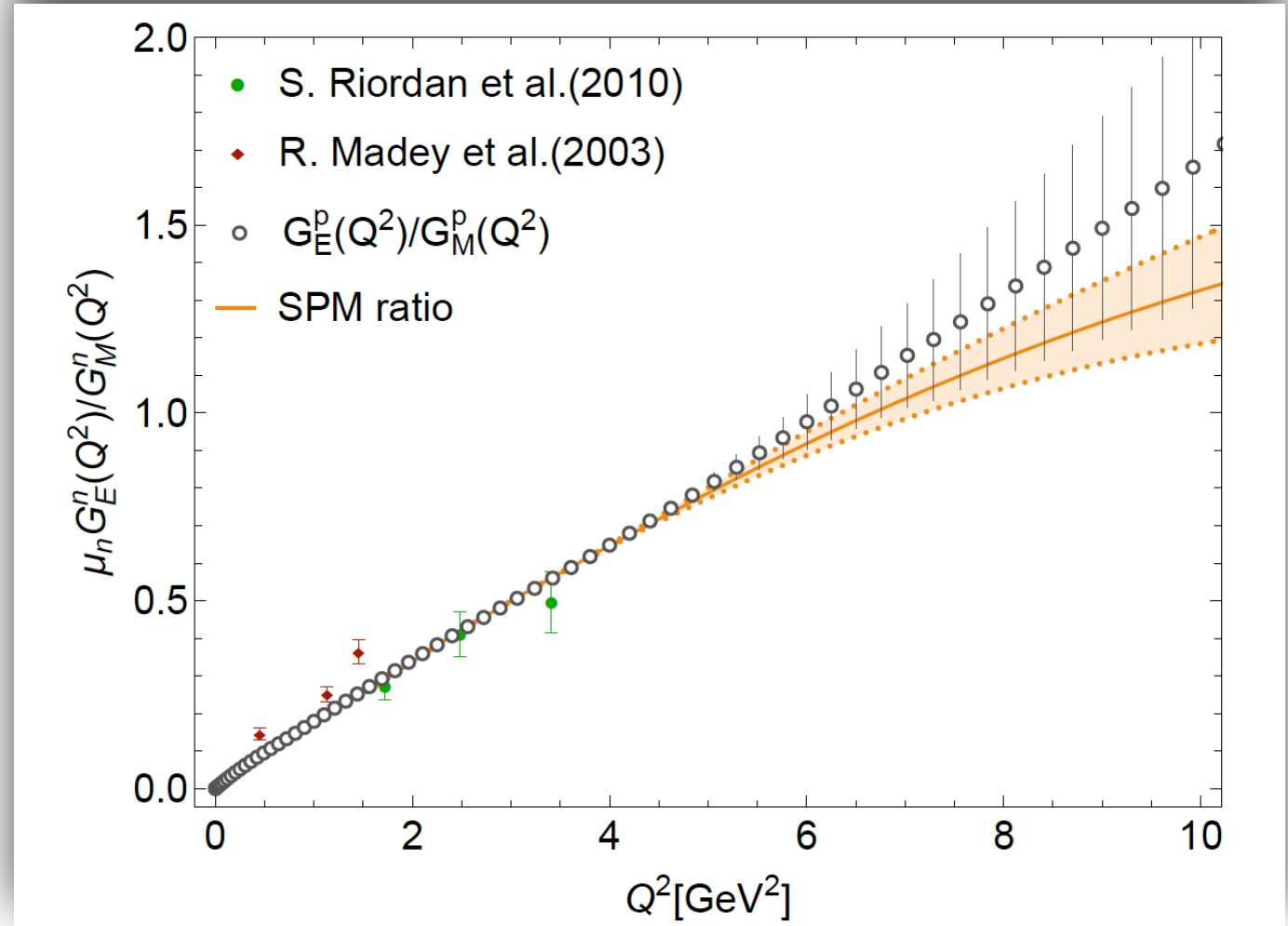
➤ Schlessinger point method (SPM) has been used for study the form factor at large Q^2 .

➤ Data at JLab show a trend toward zero with increasing momentum transfer.

➤ Ratio for proton:

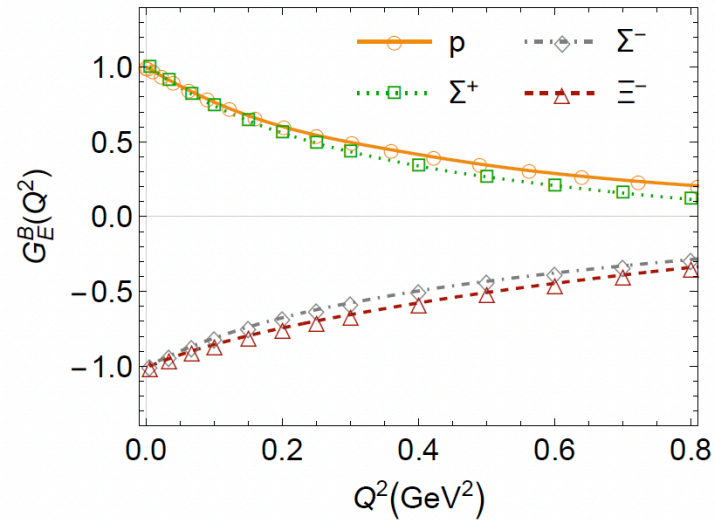
$$\frac{\mu_p G_E^p}{G_M^p} = 0 \text{ at } Q^2 = 8.42^{+3.76}_{-0.86} \text{ GeV}^2$$

➤ Ratio for neutron:

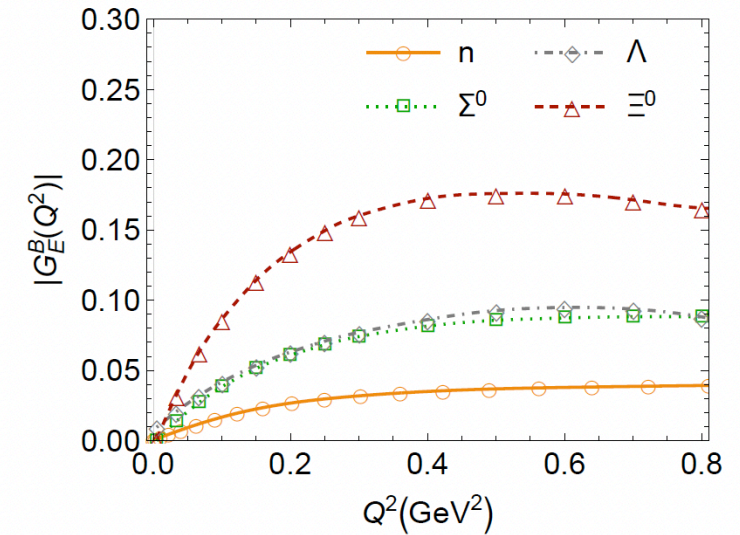


Electromagnetic form factors - octet

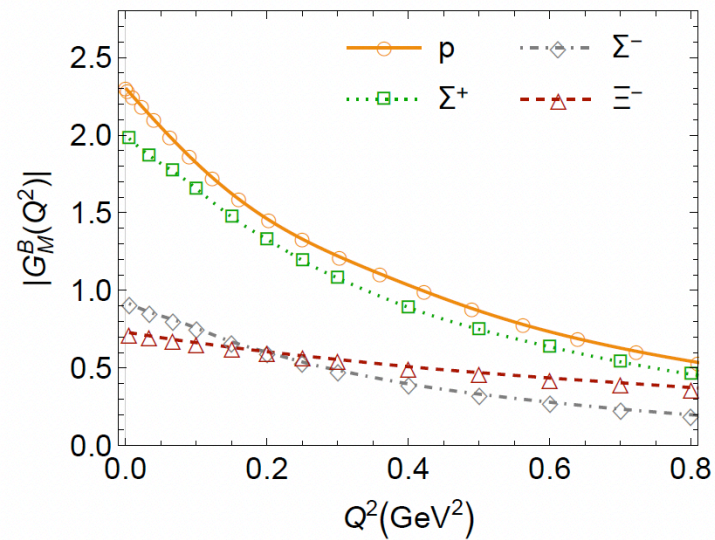
➤ Electromagnetic form factors for octet (preliminary):



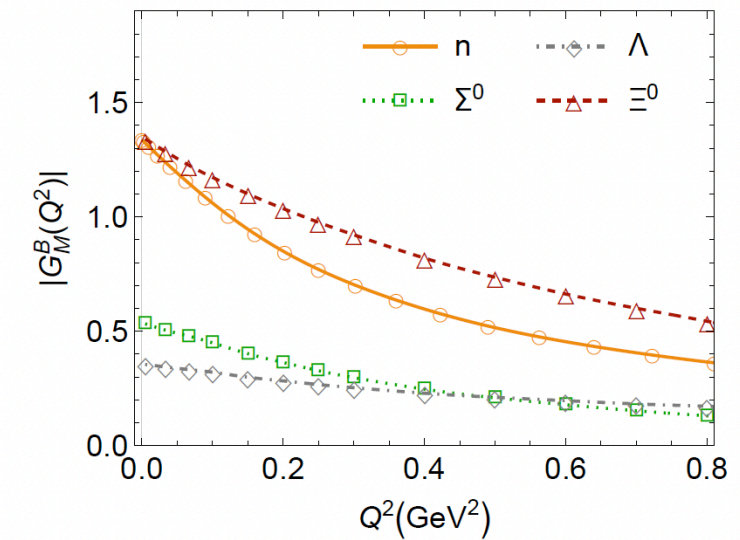
A



B



C



D

Electromagnetic form factors - magnetic moments

➤ The magnetic moments (preliminary): $\mu_B = G_M^B(Q^2 = 0)$

proton: $\mu_p = 2.30$

neutron: $\mu_n = -1.34$

Table 3: Predictions for magnetic moments $\mu_B = G_M^B(Q^2 = 0)$. The results from two lattice (lQCD), nonlocal chiral effective theory (NEFT), Chiral perturbation theory (χ PT), NJL and perturbative chiral quark model (PCQM) as well as the experimental data are also listed.

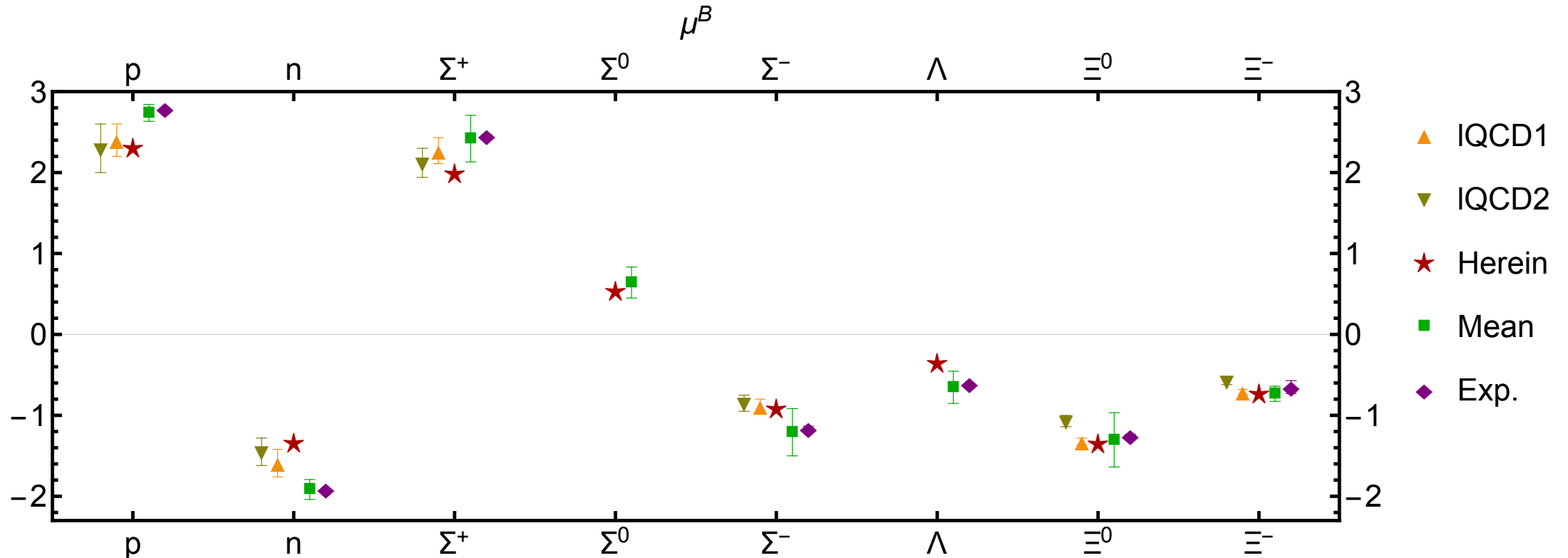
μ_B	p	n	Σ^+	Σ^0	Σ^-	Λ	Ξ^0	Ξ^-
Herein	2.30	-1.34	1.99	0.537	-0.922	-0.357	-1.35	-0.732
lQCD [24]	2.4(2)	-1.59(17)	2.27(16)	-	-0.88(8)	-	-1.32(4)	-0.71(3)
lQCD [33]	2.3(3)	-1.45(17)	2.12(18)	-	-0.85(10)	-	-1.07(7)	-0.57(5)
E [13]&S [32]	2.21(1)	-1.33(1)	1.82(2)	0.521(1)	-0.78(2)	-0.435(5)	-1.05(1)	-0.57(4)
NEFT [38]	2.644 (159)	-1.984(216)	2.421(147)	0.584 (77)	-1.253(8)	-0.594(57)	-1.380(169)	-0.725(77)
χ PT [18]	2.79	-1.913	2.1(4)	0.5(2)	-1.1(1)	-0.5(2)	-1.0(4)	-0.7(1)
NJL [7]	2.78	-1.81	2.62	-	-1.62	-	-1.14	-0.67
PCQM [25]	2.735(121)	-1.956(103)	2.537(201)	0.838(91)	-0.861(40)	-0.867(74)	-1.690(142)	-0.840(87)
Exp. [40]	2.793	-1.913	2.458(10)	-	-1.160(25)	-0.613(4)	-1.250(14)	-0.651(80)

Electromagnetic form factors - magnetic moments

➤ The magnetic moments (preliminary): $\mu_B = G_M^B(Q^2 = 0)$

proton: $\mu_p = 2.30$

neutron: $\mu_n = -1.34$



Electromagnetic form factors - charge radius

- The charge radius for charged baryon(preliminary):

$$\langle r_E^2 \rangle^B = - \frac{6}{G_E^B(0)} \frac{d}{dQ^2} G_E^B(Q^2) \Big|_{Q^2=0}$$

- The charge radius for neutral baryons(preliminary):

$$\langle r_E^2 \rangle^B = - 6 \frac{d}{dQ^2} G_E^B(Q^2) \Big|_{Q^2=0}$$

Table 5: Predictions for octet charge radii $\langle r_E^2 \rangle$. The results from two lattice(QCD), nonlocal chiral effective theory(NEFT), Chiral perturbation theory(χ PT), NJL and perturbative chiral quark model(PCQM) as well as the experimental data are also listed. All values are in units of fm^2 .

$\langle r_E^2 \rangle$	p	n	Σ^+	Σ^0	Σ^-	Λ	Ξ^0	Ξ^-
Herein	0.627	-0.0455	0.778	0.121	0.545	0.0974	0.284	0.438
lQCD [35]	0.685(66)	-0.158(33)	0.749(72)	-	0.657(58)	0.010(9)	0.082(29)	0.502(47)
lQCD [34]	0.76(10)	-	0.61(8)	-	0.45(3)	-	-	0.37(2)
E [13]&S [32]	0.56(4)	-0.01	0.56(3)	0.057(8)	0.45(3)	0.04(1)	0.10(1)	0.37(4)
NEFT [38]	0.729(112)	-0.146(18)	0.719(116)	0.010(4)	0.700 (124)	-0.015(4)	-0.015(7)	0.601(127)
χ PT [18]	0.878	0.03(7)	0.99(3)	0.10(2)	0.780	0.18(1)	0.36(2)	0.61(1)
NJL [7]	0.76	-0.14	0.92	-	0.74	-	0.24	0.58
PCQM [25]	0.767(113)	-0.014(1)	0.781(108)	-	0.781(63)	-	0.014(8)	0.767(113)
Exp. [40]	0.7070(7)	-0.1160(22)	-	-	0.61(16)	-	-	-

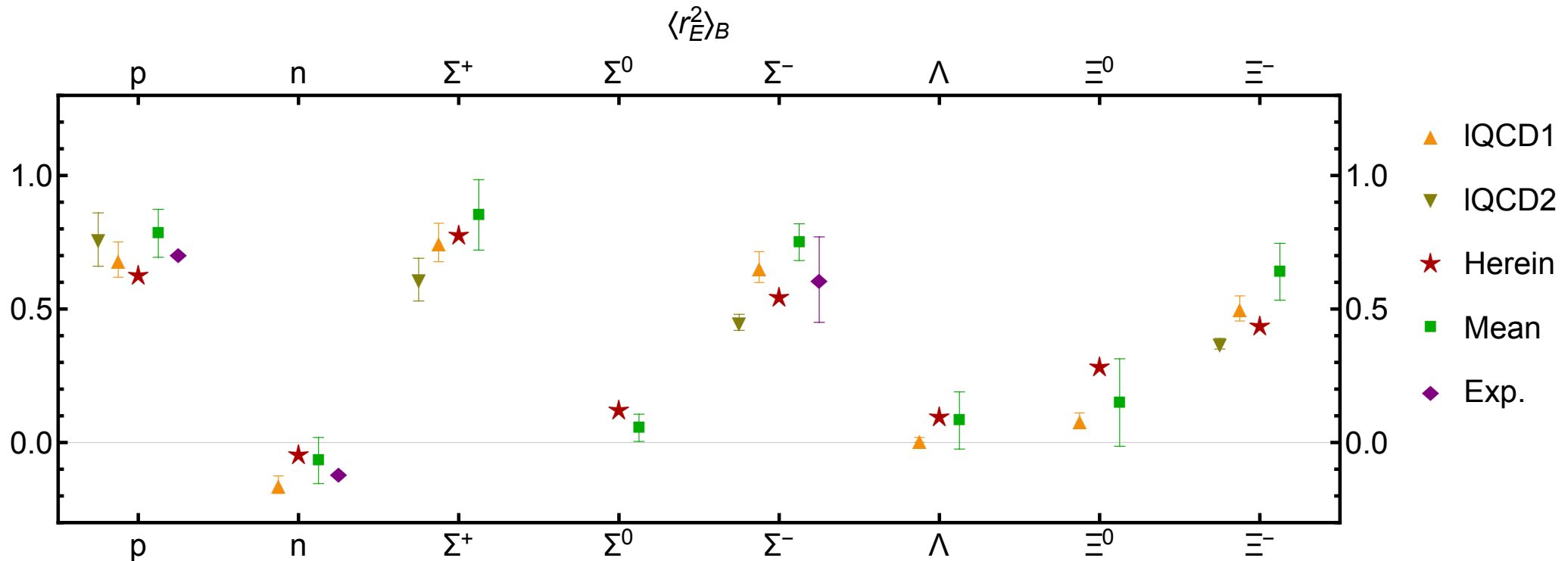
Electromagnetic form factors - charge radius

➤ The charge radius for charged baryon (preliminary):

$$\langle r_E^2 \rangle^B = - \frac{6}{G_E^B(0)} \frac{d}{dQ^2} G_E^B(Q^2) \Big|_{Q^2=0}$$

➤ The charge radius for neutral baryons (preliminary):

$$\langle r_E^2 \rangle^B = - 6 \frac{d}{dQ^2} G_E^B(Q^2) \Big|_{Q^2=0}$$



Electromagnetic form factors - magnetic radius

- The magnetic radius is in both cases as (preliminary):

$$\langle r_M^2 \rangle^B = - \frac{6}{G_M^B(0)} \frac{d}{dQ^2} G_M^B(Q^2) \Big|_{Q^2=0}$$

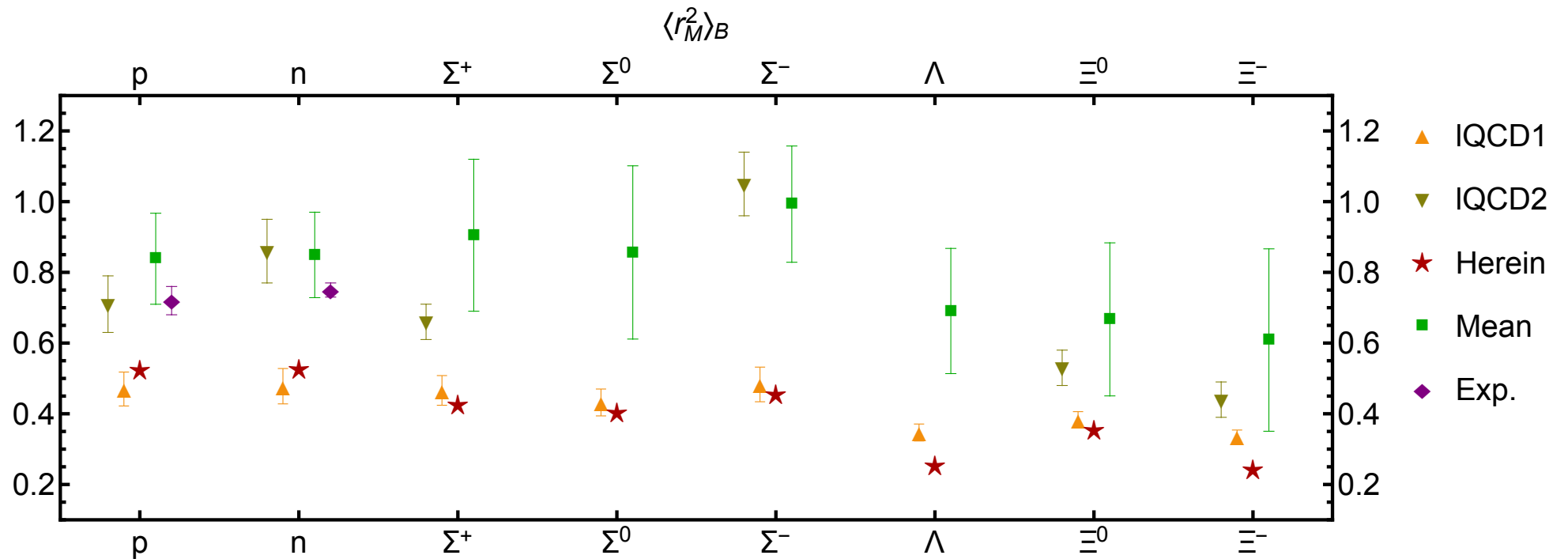
Table 5: Predictions for octet magnetic radii $\langle r_M^2 \rangle$. The results from two lattice(lQCD), nonlocal chiral effective theory(NEFT), Chiral perturbation theory(χ PT), NJL and perturbative chiral quark model(PCQM) as well as the experimental data are also listed. All values are in units of fm^2 .

$\langle r_M^2 \rangle$	p	n	Σ^+	Σ^0	Σ^-	Λ	Ξ^0	Ξ^-
Herein	0.523	0.526	0.426	0.404	0.455	0.252	0.353	0.243
lQCD [6]	0.470(48)	0.478(50)	0.466(42)	0.432(38)	0.483(49)	0.347(24)	0.384(22)	0.336(18)
lQCD [33]	0.71(8)	0.86(9)	0.66(5)	-	1.05(9)	-	0.53(5)	0.44(5)
E [13]&S [32]	0.52(3)	0.52(3)	0.43(2)	0.39(3)	0.50(1)	0.21(1)	0.35(3)	0.20(2)
NEFT [38]	0.785(132)	0.845(148)	0.765(131)	0.618(124)	0.901(119)	0.620(126)	0.657(128)	0.534(135)
χ PT [18]	0.9(2)	0.8(2)	1.2(2)	1.1(2)	1.2(2)	0.6(2)	0.7(3)	0.8(1)
NJL [7]	0.76	0.83	0.77	-	0.92	-	0.44	0.26
PCQM [25]	0.909(84)	0.922(79)	0.885(94)	0.851(102)	0.951(83)	0.852(103)	0.871(99)	0.840(109)
Exp. [40]	0.72(4)	0.75(2)	-	-	-	-	-	-

Electromagnetic form factors - magnetic radius

➤ The magnetic radius is in both cases as (preliminary):

$$\langle r_M^2 \rangle^B = - \frac{6}{G_M^B(0)} \frac{d}{dQ^2} G_M^B(Q^2) \Big|_{Q^2=0}$$



Electromagnetic form factors - magnetic/charge radius

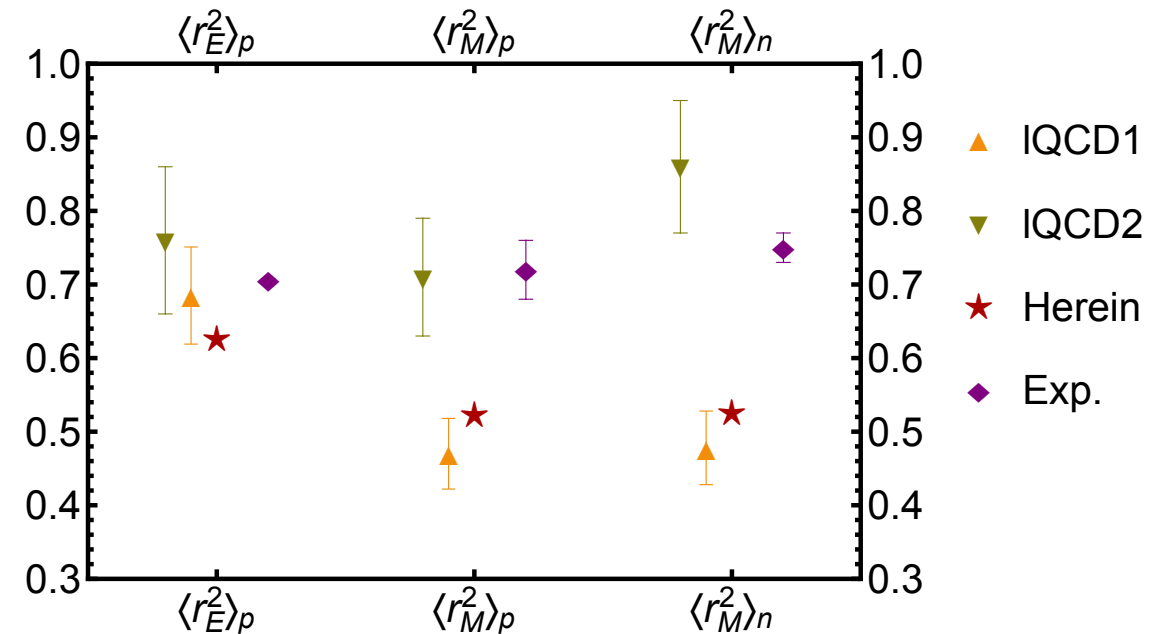
➤ The magnetic radius is in both cases as (preliminary):

$$\langle r_M^2 \rangle^B = - \frac{6}{G_M^B(0)} \frac{d}{dQ^2} G_M^B(Q^2) \Big|_{Q^2=0}$$

➤ The charge radius for charged baryon (preliminary):

$$\langle r_E^2 \rangle^B = - \frac{6}{G_E^B(0)} \frac{d}{dQ^2} G_E^B(Q^2) \Big|_{Q^2=0}$$

$\langle r_M^2 \rangle$	p	n	$\langle r_E^2 \rangle$	p
Herein	0.523	0.526	Herein	0.627
IQCD [6]	0.470(48)	0.478(50)	IQCD [35]	0.685(66)
IQCD [33]	0.71(8)	0.86(9)	IQCD [34]	0.76(10)
E [13]&S [32]	0.52(3)	0.52(3)	E [13]&S [32]	0.56(4)
NEFT [38]	0.785(132)	0.845(148)	NEFT [38]	0.729(112)
χ PT [18]	0.9(2)	0.8(2)	χ PT [18]	0.878
NJL [7]	0.76	0.83	NJL [7]	0.76
PCQM [25]	0.909(84)	0.922(79)	PCQM [25]	0.767(113)
Exp. [40]	0.72(4)	0.75(2)	Exp. [40]	0.7070(7)



Weak form factors

- The nucleon matrix elements of the axialvector and pseudoscalar current are parametrized by the axial, induced pseudoscalar form factors:

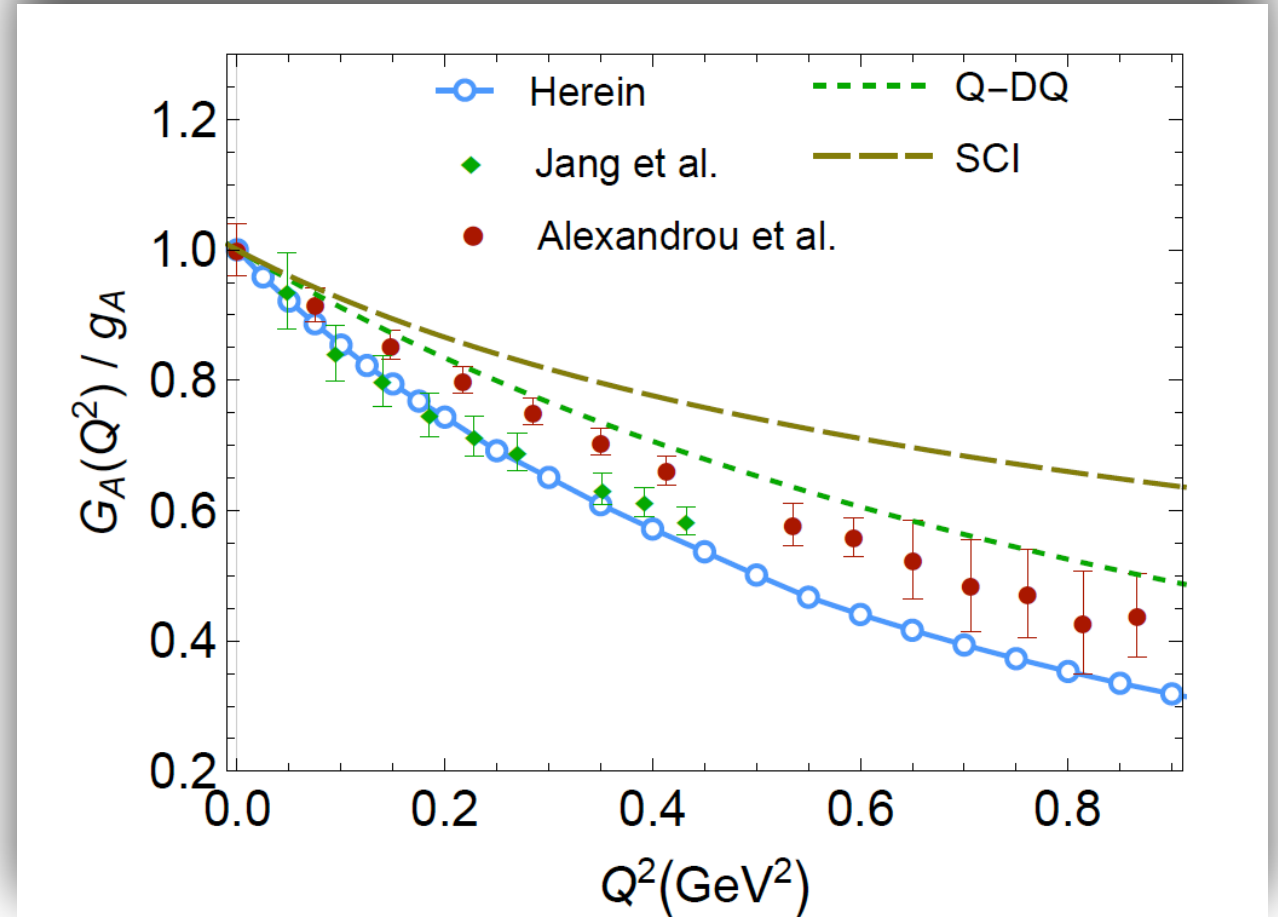
$$\begin{aligned} J_5^{\mu B'B}(P, Q) &:= \left\langle B'(p_f) \left| A_{5\mu}^{fg}(Q^2) \right| B(p_i) \right\rangle \\ &= \Lambda_+(p_f) \gamma_5 \left[\gamma_\mu G_A^{B'B}(Q^2) + \frac{iQ_\mu}{2M_{B'B}} G_P^{B'B}(Q^2) \right] \Lambda_+(p_i). \end{aligned}$$

- and pseudo-scalar form factors

$$J_5^{B'B}(P, Q) := \left\langle B'(p_i) \left| P_5^{fg}(Q^2) \right| B(p_f) \right\rangle = \Lambda_+(p_f) \gamma_5 G_5^{B'B}(Q^2) \Lambda_+(p_i).$$

neutron->proton $G_A(Q^2)$

➤ Axial form factors $G_A(Q^2)$



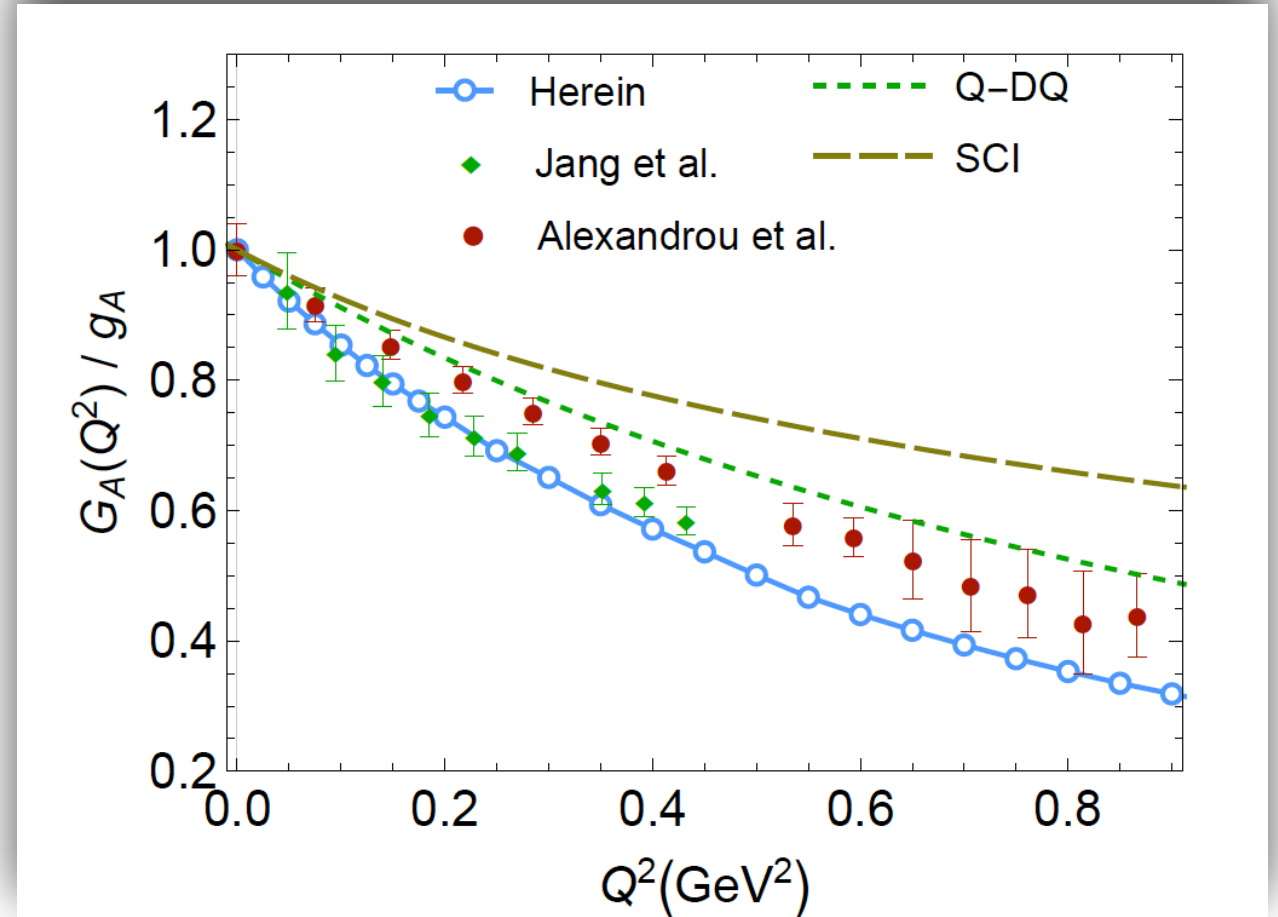
neutron->proton $G_A(Q^2)$

➤ Axial form factors $G_A(Q^2)$

➤ Our result for the axial charge

$$g_A := G_A(0) = 1.14$$

Experimental value $g_A = 1.2695(29)$ is precisely known from neutron β decay.



neutron->proton $G_A(Q^2)$

➤ Axial form factors $G_A(Q^2)$

➤ Our result for the axial charge

$$g_A := G_A(0) = 1.14$$

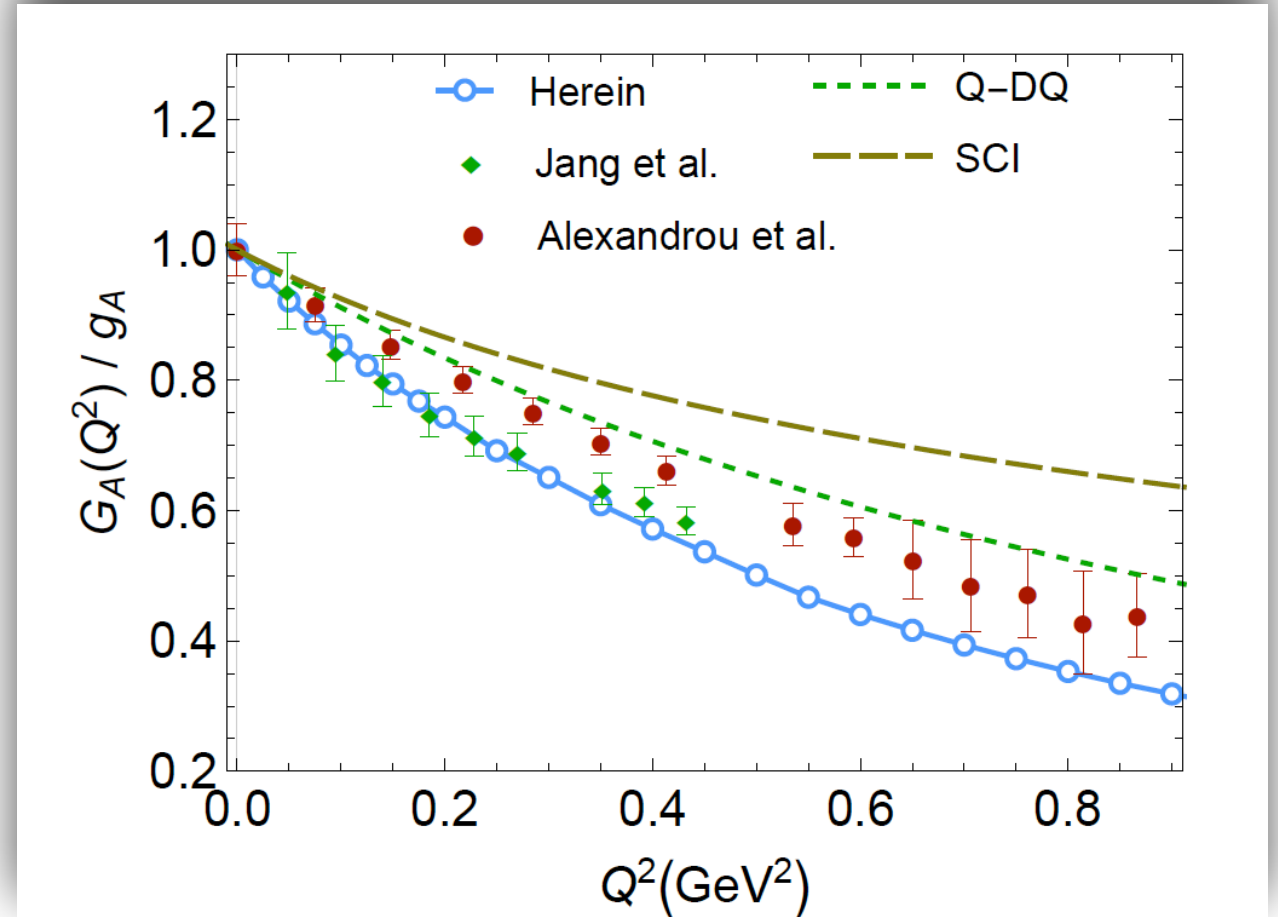
Experimental value $g_A = 1.2695(29)$ is precisely known from neutron β decay.

➤ Flavour separation of proton axial charge:

$$g_A^u := G_A^u(0) = 0.888; \quad g_A^d := G_A^d(0) = -0.247$$

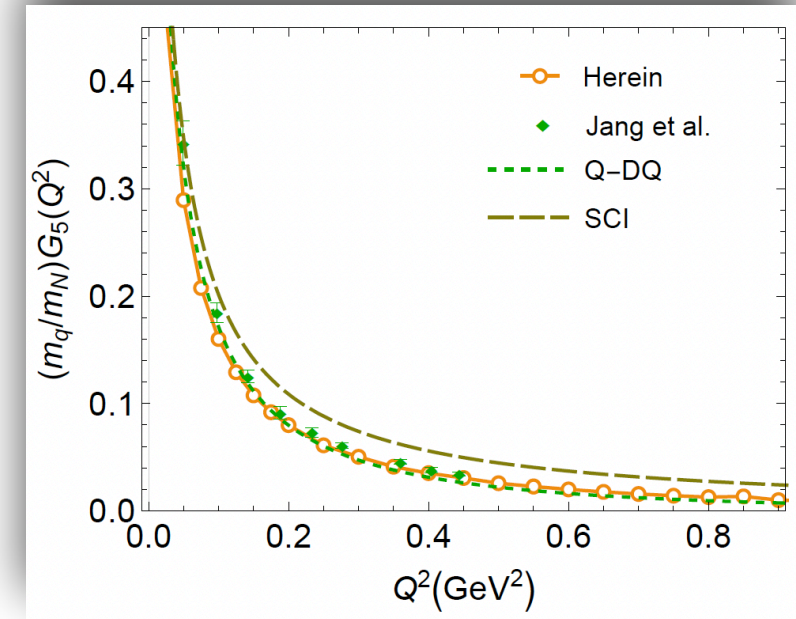
$$\text{the ratio of axial charges: } \frac{g_A^d}{g_A^u} = -0.278$$

$$\text{Experiment: } \frac{g_A^d}{g_A^u} = -0.27(4)$$



neutron->proton $G_P(Q^2)$ & $G_5(Q^2)$

➤ Pseudoscalar form factor $G_5(Q^2)$



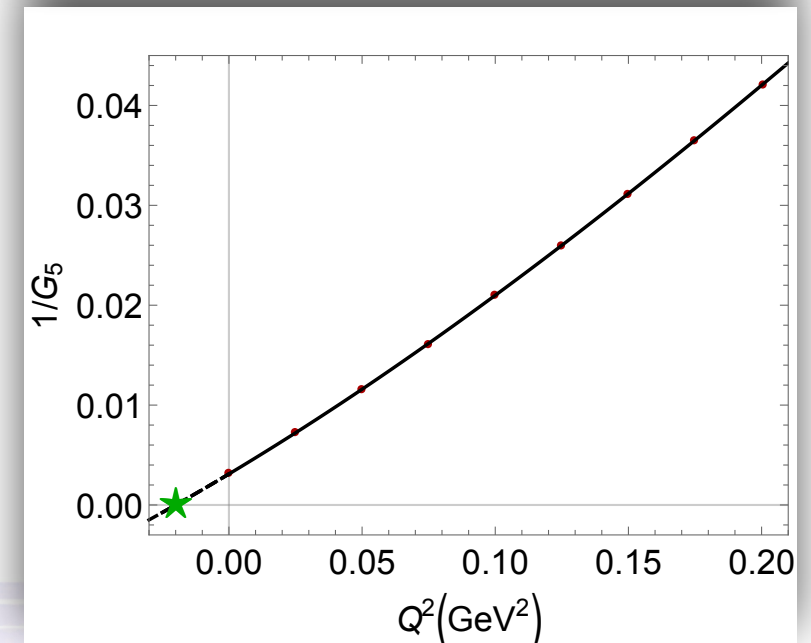
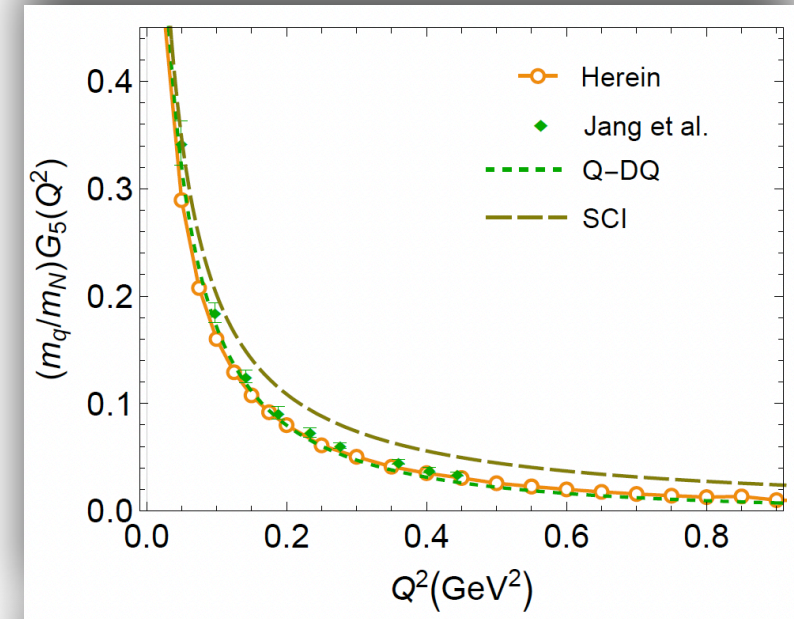
neutron->proton $G_P(Q^2)$ & $G_5(Q^2)$

➤ Pseudoscalar form factor $G_5(Q^2)$

➤ The pion-nucleon form factor $G_{\pi NN}(Q^2)$

$$G_{\pi NN}(Q^2) \frac{f_\pi}{m_N} \frac{m_\pi^2}{Q^2 + m_\pi^2} = \frac{m_l}{m_N} G_5^{pn}(Q^2)$$

The extrapolation of $1/G_5(Q^2)$ from the space-like region onto a small domain of time-like momenta shows $G_5(Q^2)$ has a pole at the on-shell pion mass.



neutron->proton $G_P(Q^2)$ & $G_5(Q^2)$

➤ Pseudoscalar form factor $G_5(Q^2)$

➤ The pion-nucleon form factor $G_{\pi NN}(Q^2)$

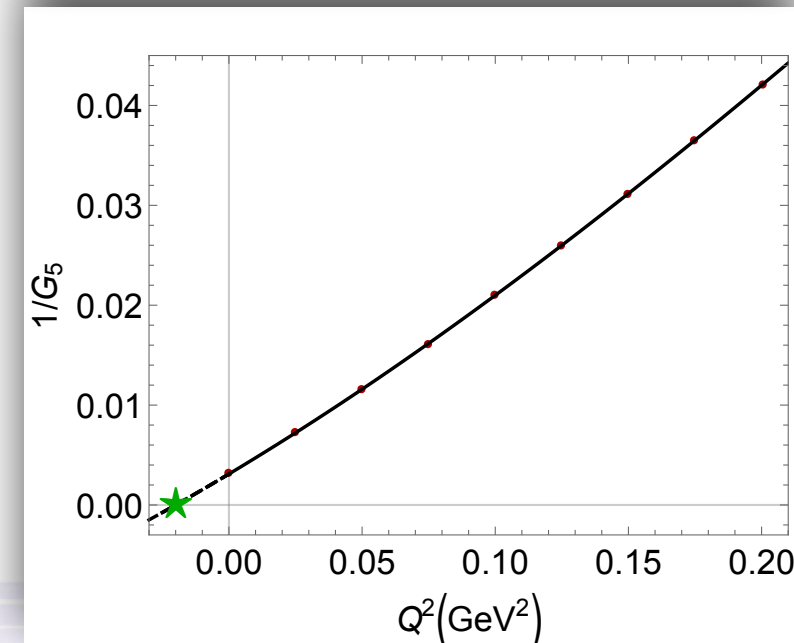
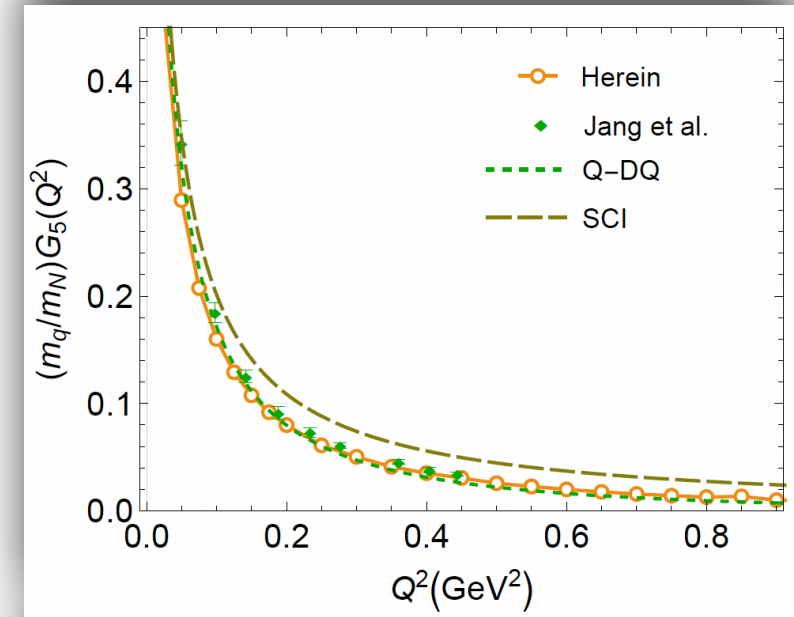
$$G_{\pi NN}(Q^2) \frac{f_\pi}{m_N} \frac{m_\pi^2}{Q^2 + m_\pi^2} = \frac{m_l}{m_N} G_5^{pn}(Q^2)$$

The extrapolation of $1/G_5(Q^2)$ from the space-like region onto a small domain of time-like momenta shows $G_5(Q^2)$ has a pole at the on-shell pion mass.

➤ Pion-nucleon coupling constant $g_{\pi NN}$ is the residue of $G_5(Q^2)$ at $Q^2 + m_\pi^2 = 0$

$$g_{\pi NN} \frac{f_\pi}{m_N} = \lim_{Q^2 + m_\pi^2 \rightarrow 0} (1 + Q^2/m_\pi^2) \frac{m_l}{m_N} G_5^{pn}(Q^2)$$

Our prediction: $g_{\pi NN} = 11.99$



neutron->proton $G_P(Q^2)$ & $G_5(Q^2)$

- Ward-Green-Takahashi identities at the nucleon level become

$$Q^\mu J_5^\mu + 2m_q J_5 = 0$$

- Goldberger-Treiman relation at the form factor level

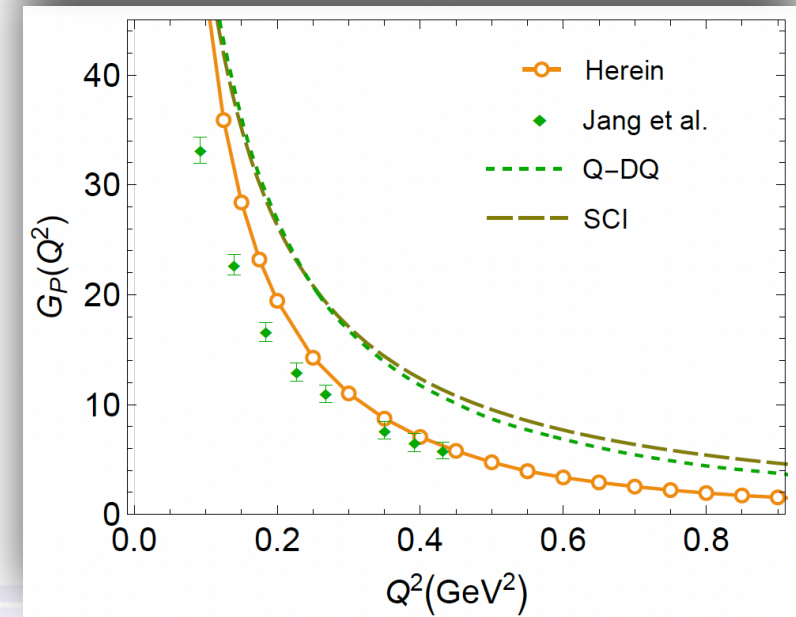
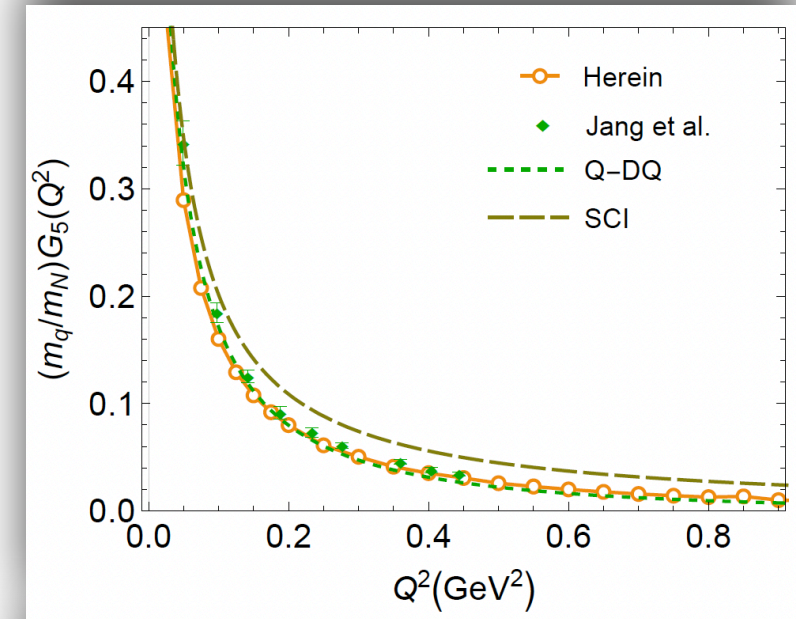
$$G_A^{pn}(0) = \frac{m_l}{m_N} G_5^{pn}(0)$$

Herein,

$$G_A^{pn}(0) = 1.17$$

$$\frac{m_l}{m_N} G_5^{pn}(0) = 1.14$$

The error is less than 5%.

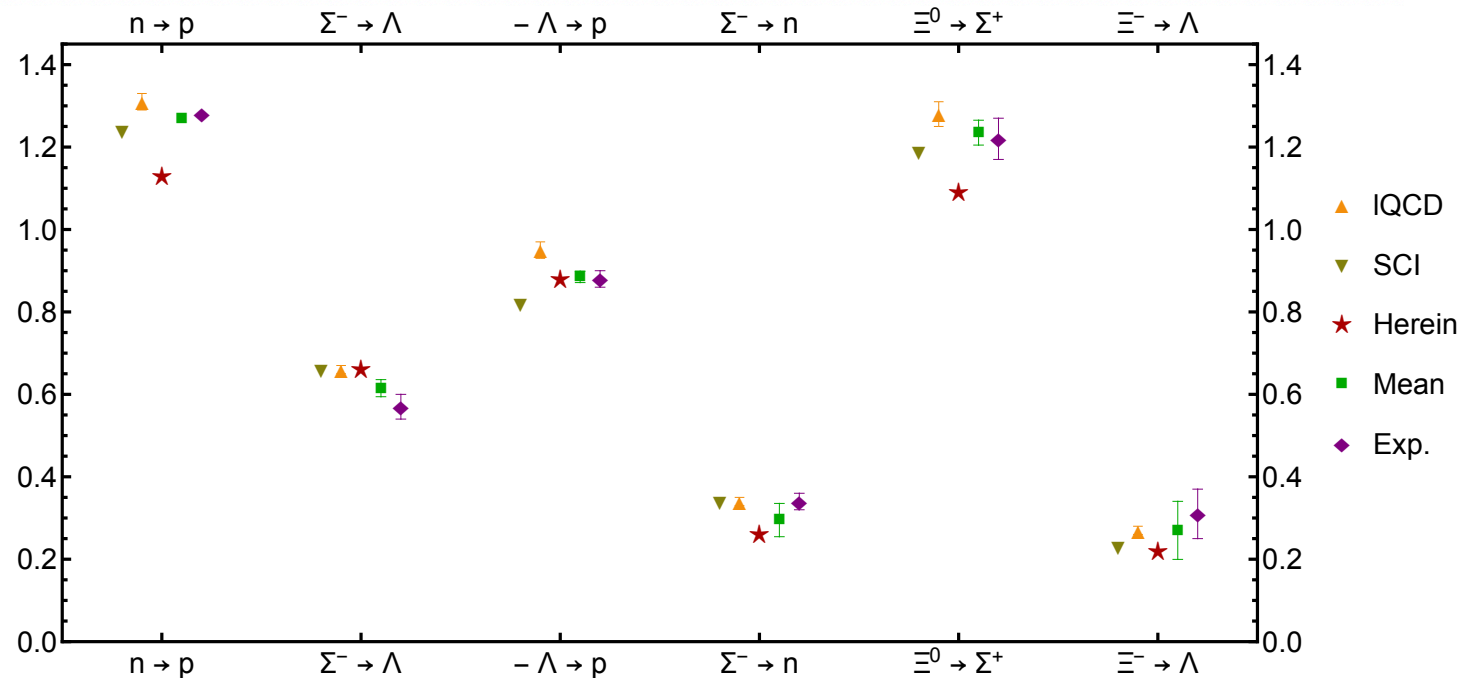


Axial form factors

➤ Our result for the axial charge (preliminary)

$$g_A^B := G_A^B(Q^2=0):$$

	$n \rightarrow p$	$\Sigma^- \rightarrow \Lambda$	$\Lambda \rightarrow p$	$\Sigma^- \rightarrow n$	$\Xi^0 \rightarrow \Sigma^+$	$\Xi^- \rightarrow \Lambda$
Herein	1.13	0.661	-0.879	0.260	1.09	0.219
lQCD [37]	1.31(2)	0.66(1)	-0.95(2)	0.34(1)	1.28(3)	0.27(1)
SCI [10]	1.24	0.66	-0.82	0.34	1.19	0.23
QM [14]	1.27	0.63	-0.89	0.26	1.25	0.33
χ PT [23]	1.27	0.60(2)	-0.88(2)	0.33(2)	1.22(4)	0.21(4)
Exp. [40]	1.28	0.57(3)	-0.88(2)	0.34(2)	1.22(5)	0.31(6)



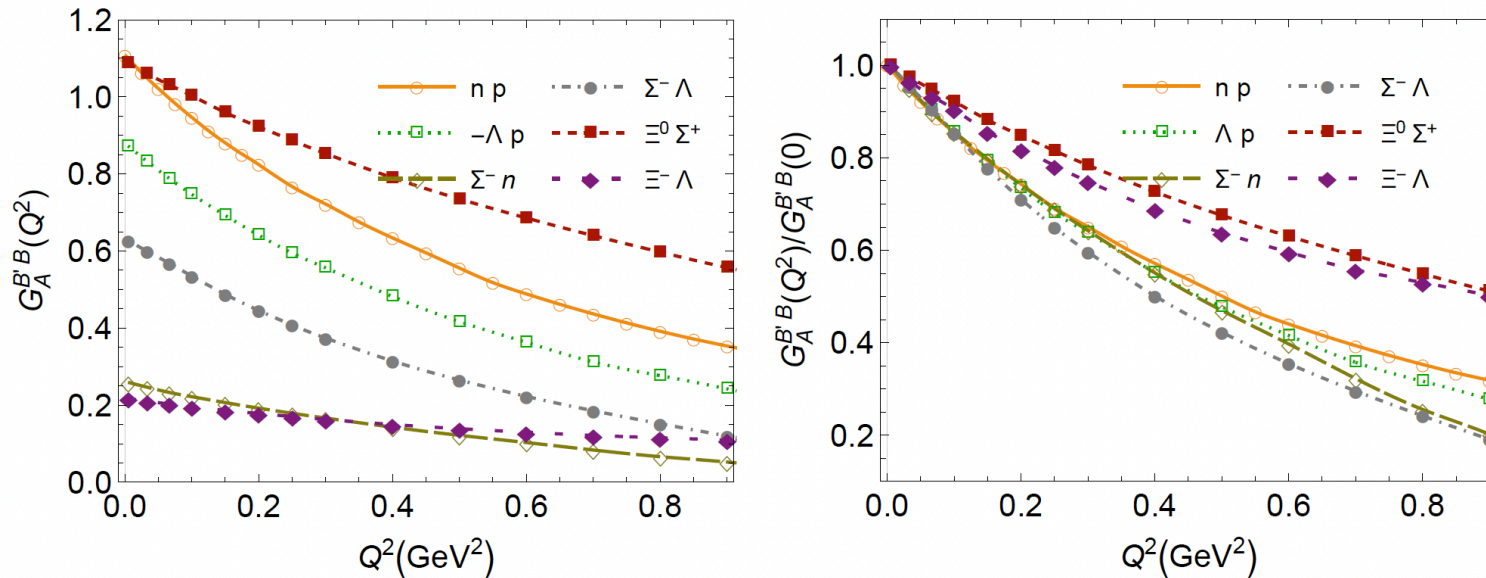
Axial form factors

➤ Our result for the axial charge (preliminary)

$$g_A^B := G_A^B(Q^2=0):$$

	$n \rightarrow p$	$\Sigma^- \rightarrow \Lambda$	$\Lambda \rightarrow p$	$\Sigma^- \rightarrow n$	$\Xi^0 \rightarrow \Sigma^+$	$\Xi^- \rightarrow \Lambda$
Herein	1.13	0.661	-0.879	0.260	1.09	0.219
lQCD [37]	1.31(2)	0.66(1)	-0.95(2)	0.34(1)	1.28(3)	0.27(1)
SCI [10]	1.24	0.66	-0.82	0.34	1.19	0.23
QM [14]	1.27	0.63	-0.89	0.26	1.25	0.33
χ PT [23]	1.27	0.60(2)	-0.88(2)	0.33(2)	1.22(4)	0.21(4)
Exp. [40]	1.28	0.57(3)	-0.88(2)	0.34(2)	1.22(5)	0.31(6)

➤ The axial form factors $G_A^B(Q^2)$ (preliminary):



Outlook

Based on Faddeev equation, we can study

- spectrum/structure of decuplet baryons;
- nucleon gravitational form factors
- octet beyond rainbow-ladder truncation
- PDAs/PDFs of baryons;
- hybrid meson.....

Outlook

Based on Faddeev equation, we can study

- spectrum/structure of decuplet baryons;
- nucleon gravitational form factors
- octet beyond rainbow-ladder truncation
- PDAs/PDFs of baryons;
- hybrid meson.....

CHIN. PHYS. LETT. Vol. 38, No. 7 (2021) 071201

Express Letter

Resolving the Bethe–Salpeter Kernel

Si-Xue Qin(秦思学)^{1*} and Craig D. Roberts^{2,3*}

¹Department of Physics, Chongqing University, Chongqing 401331, China

²School of Physics, Nanjing University, Nanjing 210093, China

³Institute for Nonperturbative Physics, Nanjing University, Nanjing 210093, China

(Received 18 May 2021; accepted 25 May 2021; published online 6 June 2021)

A novel method for constructing a kernel for the meson bound-state problem is described. It produces a closed form that is symmetry-consistent (discrete and continuous) with the gap equation defined by any admissible gluon-quark vertex, Γ . Applicable even when the diagrammatic content of Γ is unknown, the scheme can foster new synergies between continuum and lattice approaches to strong interactions. The framework is illustrated by showing that the presence of a dressed-quark anomalous magnetic moment in Γ , an emergent feature of strong interactions, can remedy many defects of widely used meson bound-state kernels, including the mass splittings between vector and axial-vector mesons and the level ordering of pseudoscalar and vector meson radial excitations.

DOI: 10.1088/0256-307X/38/7/071201

Outlook

Based on Faddeev equation, we can study

- spectrum/structure of decuplet baryons;
- nucleon gravitational form factors
- octet beyond rainbow-ladder truncation
- PDAs/PDFs of baryons;
- hybrid meson.....

Summary

- Direct solution of Faddeev equation using rainbow-ladder truncation is now possible.
- octet spectrum
- Electromagnetic form factors for octet
 - zero of ratio $\frac{\mu_p G_E^p}{G_M^p} = 0$ at $Q^2 = 8.42^{+3.76}_{-0.86} \text{GeV}^2$
 - magnetic moments
 - charge & magnetic radius
- Weak form factors for octet
 - $G_A(Q^2): g_A=1.14$
 - the ratio of axial charges: $\frac{g_A^d}{g_A^u} = -0.278$; experiment: $\frac{g_A^d}{g_A^u} = -0.27(4)$
 - $G_5(Q^2): g_{\pi NN}=11.99$

Thank You!

Baryons' octet spectrum

$$\psi_{\alpha\beta\gamma\mathcal{I}}^{\mathcal{M}_A}(p, q, P) = \sum_{a=1}^3 \int_k \sum_i^{d_F^A} S_{\alpha'\alpha''}^{\lambda_{a_r}^i}(k_1) S_{\beta'\beta''}^{\lambda_{a_l}^i}(\tilde{k}_2) \psi_{\alpha'\beta'\gamma\mathcal{I}}^{\mathcal{M}_A}(p^{(a)}, q^{(a)}, P);$$



$$\psi_{\alpha\beta\gamma\mathcal{I}}^{\mathcal{M}_S}(p, q, P) = \sum_{a=1}^3 \int_k \sum_i^{d_F^S} S_{\alpha'\alpha''}^{\lambda_{a_r}^i}(k_1) S_{\beta'\beta''}^{\lambda_{a_l}^i}(\tilde{k}_2) \psi_{\alpha'\beta'\gamma\mathcal{I}}^{\mathcal{M}_S}(p^{(a)}, q^{(a)}, P),$$

- For the proton and neutron, isospin symmetry makes: $S^u = S^d$

$$m_{\mathcal{M}_A} \equiv m_{\mathcal{M}_S}$$

	N	$\Lambda(uds)$	$\Sigma(uus)$	$\Xi(uss)$
Herein(\mathcal{M}_A)	0.938	1.065	1.113	1.345
Herein(\mathcal{M}_S)	0.938	1.077	1.117	1.320
Herein(<i>Mean</i>)	0.938	1.071	1.115	1.333
E [13]&S [31]	0.94	1.073(1)	1.073 (1)	1.235(5)
expt. or lQCD	0.94	1.116	1.189	1.315

Baryons' octet spectrum

$$\psi_{\alpha\beta\gamma\mathcal{I}}^{\mathcal{M}_A}(p, q, P) = \sum_{a=1}^3 \int_k \sum_i^{d_F^A} S_{\alpha'\alpha''}^{\lambda_{ar}^i}(k_1) S_{\beta'\beta''}^{\lambda_{a1}^i}(\tilde{k}_2) \psi_{\alpha'\beta'\gamma\mathcal{I}}^{\mathcal{M}_A}(p^{(a)}, q^{(a)}, P);$$



$$\psi_{\alpha\beta\gamma\mathcal{I}}^{\mathcal{M}_S}(p, q, P) = \sum_{a=1}^3 \int_k \sum_i^{d_F^S} S_{\alpha'\alpha''}^{\lambda_{ar}^i}(k_1) S_{\beta'\beta''}^{\lambda_{a1}^i}(\tilde{k}_2) \psi_{\alpha'\beta'\gamma\mathcal{I}}^{\mathcal{M}_S}(p^{(a)}, q^{(a)}, P),$$

- For the proton and neutron, isospin symmetry makes: $S^u = S^d$

$$m_{\mathcal{M}_A} \equiv m_{\mathcal{M}_S}$$

- For the remaining octet baryons

$$m_{\mathcal{M}_A} \neq m_{\mathcal{M}_S}$$

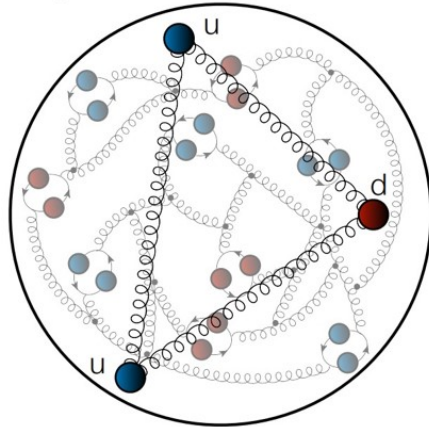
due to the SU(3) flavor breaking owing to the strange quark.

	N	$\Lambda(uds)$	$\Sigma(uus)$	$\Xi(uss)$
Herein(\mathcal{M}_A)	0.938	1.065	1.113	1.345
Herein(\mathcal{M}_S)	0.938	1.077	1.117	1.320
Herein(<i>Mean</i>)	0.938	1.071	1.115	1.333
E [13]&S [31]	0.94	1.073(1)	1.073 (1)	1.235(5)
expt. or lQCD	0.94	1.116	1.189	1.315

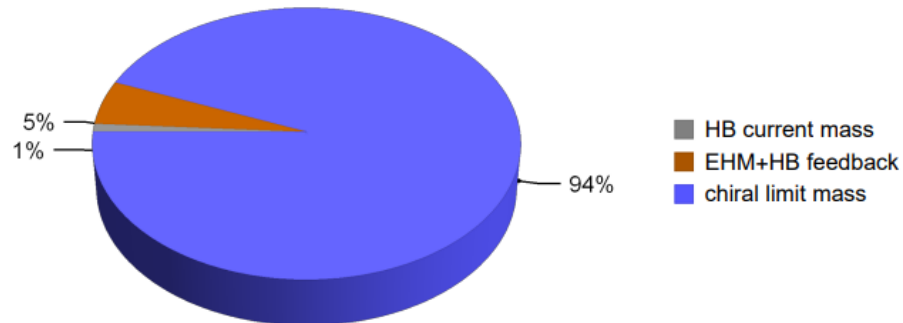
Strong interaction

- Proton valence quark: two u -quark, one d -quark.

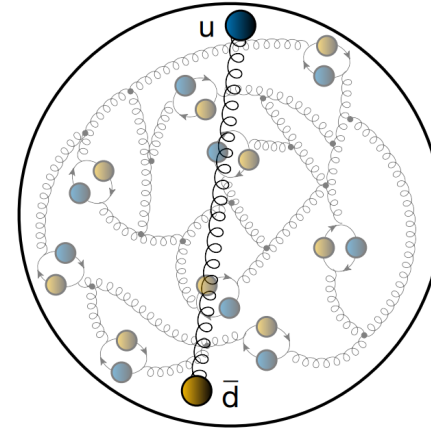
A proton



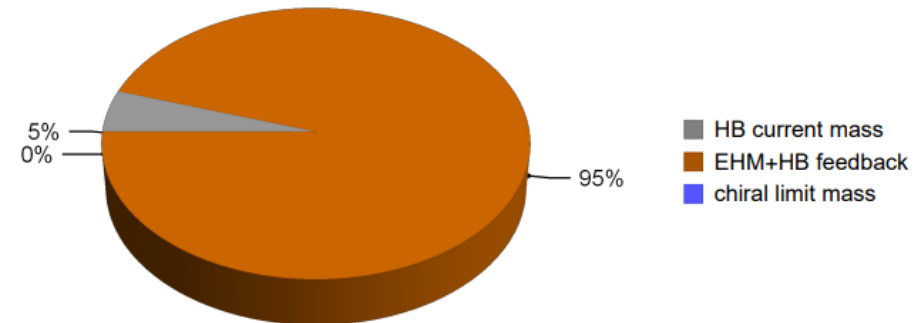
proton mass dudget



- Pion valence quark: one u -quark, one d -quark.



pion mass dudget



Strong interaction

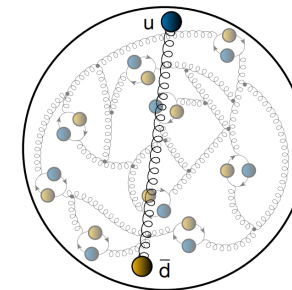
Ya Lu, et al

Phys.Lett.B 830 (2022) 1371

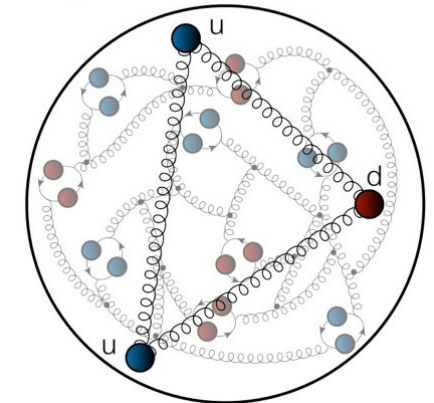
30

Nevertheless, understanding the nucleon's structure in terms of quarks and gluons, the elementary degrees of freedom of quantum chromodynamics (QCD), has remained a challenge in theoretical hadron physics.

Pion contains one valence u -quark, one valence \bar{d} -quark, and infinitely many gluons and sea quarks. These quarks are bound together by the strong interactions, described by quantum chromodynamics (QCD).



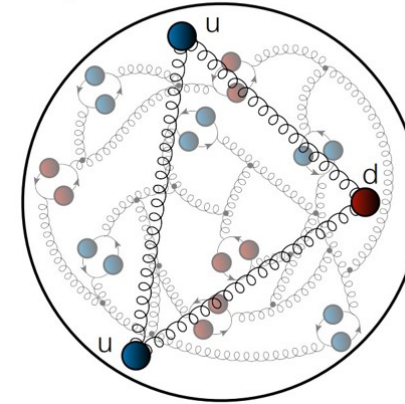
A proton



Strong interaction

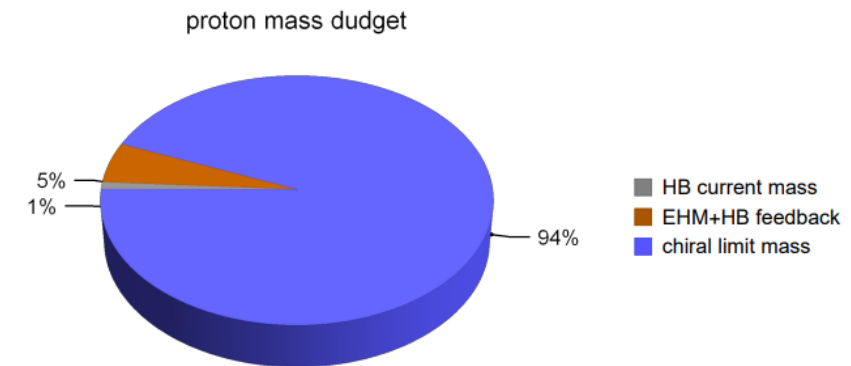
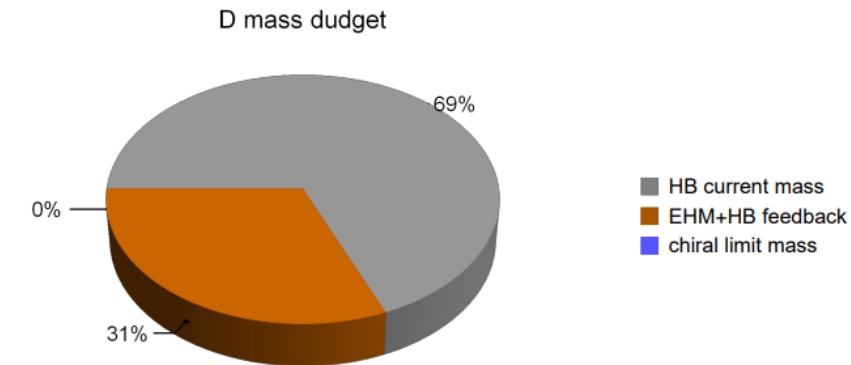
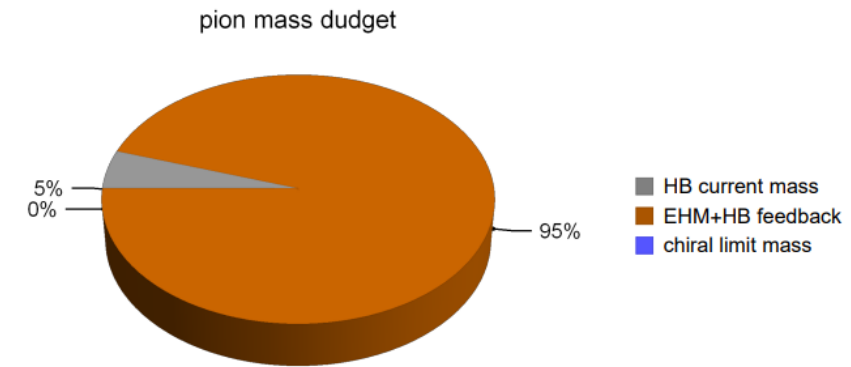
Proton contains two valence u -quark, one valence d -quark, and infinitely many gluons and sea quarks. These quarks are bound together by the strong interactions, described by quantum chromodynamics (QCD).

A proton



EHM with Semileptonic decay

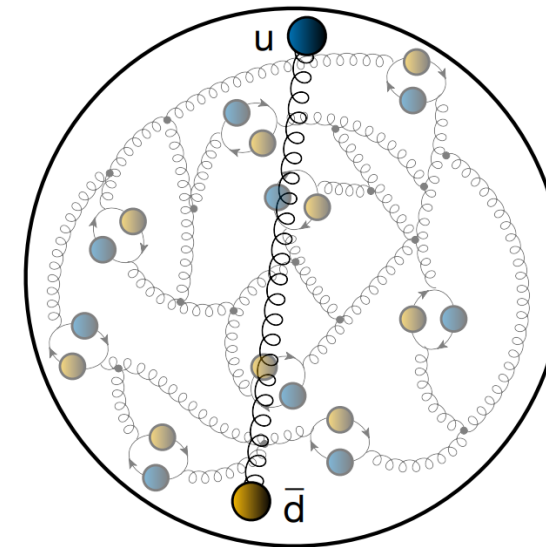
- p
 - The grey wedge in shows the sum of the valence-quark current-masses: the sum amounts to just $0.01 \times m_p$. The orange expresses the fraction of m_p generated by constructive interference between EHM and Higgs-boson (HB) effects.
- Pion - (pseudo)-Goldstone boson
 - EHM+HB interference is seen to be responsible for 95% of the pion mass.
- D meson - heavy+light meson
 - The sum of valence-quark and -antiquark current-masses in the D (heavy-light) meson accounts for 69% of its measured mass, which is 14 times more than in the pion.
- The decay of heavy-light meson to (pseudo)-Goldstone boson embodies the change of the dominate mechanism from the Higgs-related mass generation to the **EHM** in the Standard Model.



Strong interaction

Pion contains one valence u -quark, one valence \bar{d} -quark, and infinitely many gluons and sea quarks. These quarks are bound together by the strong interactions, described by quantum chromodynamics (QCD).

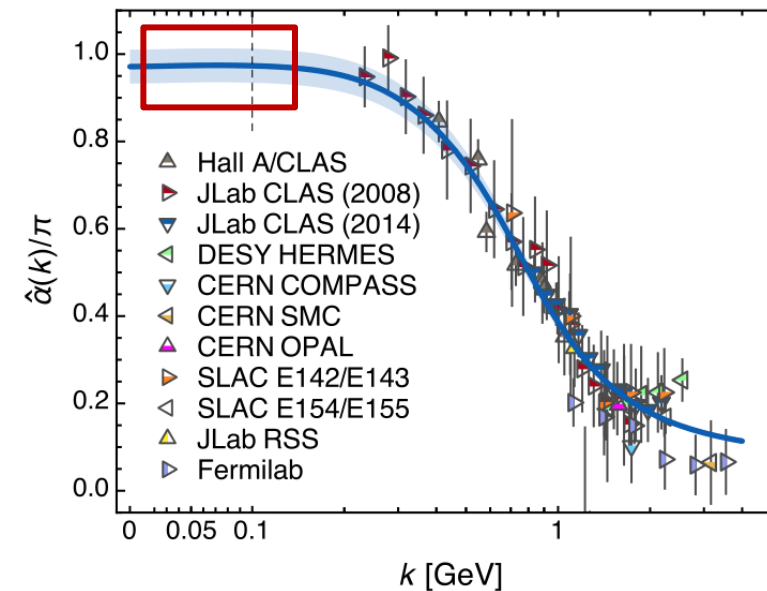
These interactions are hard for people to make predictions with perturbative approaches due to the large coupling at the typical energy scales in low energy.



Ya Lu, et al

Phys.Lett.B 830 (2022) 137130

Z.-F. Cui et al 2020 *Chinese Phys. C* 44 083102



QCD's Running Coupling